Andean Geology 37 (2): 253-275. July, 2010

Andean Geology
formerly Revista Geológica de Chile
www.scielo.cl/andgeol.htm

SHRIMP chronology of the Magallanes Basin basement, Tierra del Fuego: Cambrian plutonism and Permian high-grade metamorphism

Francisco Hervé[1], Mauricio Calderón[1], C. Mark Fanning[2], Stefan Kraus[3], Robert J. Pankhurst[4]

[1] *Departamento de Geología, Universidad de Chile, Casilla 13518, Correo 21, Santiago, Chile.*
fherve@cec.uchile.cl; caldera@esfera.cl

[2] *Research School of Earth Sciences, Australian National University, Mills Road, Canberra, ACT 0200, Australia.*
Mark.Fanning@anu.edu.au

[3] *Instituto Antártico Chileno, Plaza Muñoz Gamero 1055, Punta Arenas, Chile.*
skraus@inach.cl

[4] *NERC Isotope Geosciences Laboratory, Kingsley Dunham Centre, Keyworth, Nottingham NG12 5GG, United Kingdom.*
rjpt@nigl.nerc.ac.uk

ABSTRACT. Five new SHRIMP U-Pb zircon ages are reported for gneisses and foliated plutonic rocks belonging to the Tierra del Fuego igneous and metamorphic basement complex (TFIMC), obtained from the bottom of borehole cores through the Magallanes Basin. Three of the samples yielded weighted mean $^{206}Pb/^{238}U$ ages (523±7 Ma, 522±6 Ma and 538±6 Ma), interpreted as indicating Early Cambrian igneous crystallization of the host rocks. A migmatitic gneiss shows peaks at *ca.* 950-1,100 Ma and 560-650 Ma from inherited zircon grains in addition to two grains with ages of *ca.* 525 Ma, suggesting involvement of Grenvillian and Brasiliano material in the protolith of a Cambrian migmatite. A cordierite-sillimanite-garnet gneiss contains igneous zircons of Cambrian age and a population of U-rich metamorphic Permian zircons, indicating that a Permian high-grade metamorphic and anatectic (P=2-3 kbar, T=730-770°C) event affected the Cambrian igneous rocks or sedimentary rocks derived from them. Cambrian/Ediacaran plutonic rocks are known from the basement of NW Argentina, the Sierra de la Ventana, the Cape Fold Belt in South Africa, and the Ross Orogen in Antarctica. The Permian metamorphic event is coeval with the deformation and low-grade metamorphism of the sedimentary successions that overlie the basement in many of these areas. In Tierra del Fuego at least 8 to 12 km of cover rocks were removed following the high-grade Permian metamorphic episode and the unconformable deposition of the Tobífera Formation volcanic rocks in the Middle to Late Jurassic. This eroded cover could have been an important source of detritus for the conglomeratic Permian and Triassic? successions of neighbouring regions in South America, Africa and Antarctica.

Keywords: Cambrian plutonism, Permian metamorphism, U-Pb SHRIMP ages, Basement complex, Magallanes Basin.

RESUMEN Geocronología SHRIMP del basamento de la Cuenca de Magallanes, Tierra del Fuego: plutonismo Cámbrico y metamorfismo Pérmico de alto grado. Cinco nuevas edades radiométricas logradas mediante análisis U-Pb en circón utilizando el SHRIMP, fueron determinadas en gneises y rocas plutónicas foliadas obtenidas desde el fondo de pozos de sondajes en la Cuenca de Magallanes y pertenecientes al denominado Complejo Ígneo y Metamórfico de Tierra del Fuego. En tres de las muestras fueron calculadas edades del Cámbrico Temprano (523±7 Ma, 522±6 Ma y 538±6 Ma), interpretadas como edades de cristalización ígnea de las rocas estudiadas. Un gneis migmatítico presenta 'peaks' de circones heredados de *ca.* 950-1.100 Ma y de 560-650 Ma además de dos granos de edades de 525 Ma, indicando la participación de material Grenviliano y Brasiliano en el protolito de la migmatita cámbrica. Un gneiss de cordierita-sillimanita-granate presenta una población de circones ígneos de edad cámbrica y otro grupo de circones metamórficos, ricos en U, de edad pérmica, indicando que en el Pérmico un evento metamórfico del alto grado acompañado de anatexis (P=2-3 kbar, T=730-770°C) afectó a rocas ígneas cámbricas y/o a rocas sedimentarias derivadas de ellas. Rocas plutónicas cámbricas/ediacaranas han sido descritas en el NW de Argentina, en los basamentos de la Sierra de la Ventana y del Cinturón Plegado del Cabo (en el sur de África), y en el Orógeno de Ross en Antártica. El evento metamórfico Pérmico es contemporáneo con la deformación y metamorfismo de bajo grado, registrado en las sucesiones sedimentarias que sobreyacen el basamento en muchas de estas áreas. Siguiendo al episodio Pérmico de metamorfismo de alto grado, en Tierra del Fuego fueron removidos al menos 8 a 12 km de rocas de cobertura antes de la depositación de las rocas volcánicas de la Formación Tobífera en el Jurásico Medio y Superior. Las rocas erosionadas representan una fuente importante de material para las sucesiones conglomerádicas pérmicas y triásicas? ubicadas en las regiones vecinas de América del Sur, África y Antártica.

Palabras clave: Plutonismo Cámbrico, Metamorfismo Pérmico, Edades U-Pb SHRIMP, Complejo de basamento, Cuenca de Magallanes.

1. Introduction

The Magallanes Basin developed in Mesozoic and Cenozoic times, extending over most of Tierra del Fuego and the adjoining mainland areas of southernmost South America. The evolution of the basin began with a Middle to Late Jurassic extensional phase, which generated half grabens that were filled first with sediments and then with silicic volcanic rocks of the Tobífera Formation. Subsequent thrusting over the mainland of the quasi-oceanic Rocas Verdes basin, which developed during this extensional phase in the Pacific continental margin, generated during mid-Cretaceous to late Cenozoic times a foreland basin filled by a km-thick sedimentary succession.

The basement of this basin, except for a thin strip of low grade metasedimentary rocks at the NW coast of Peninsula Brunswick, does not crop out and is only attainable through drilling. The Tobífera Formation unconformably covers a complex of granitoids and orthogneisses, here named the Tierra del Fuego Igneous and Metamorphic Complex (TFIMC). The age of this pre-Middle Jurassic unit has been difficult to ascertain with Rb-Sr and K-Ar techniques. From the U-Pb data of Söllner *et al.* (2000) and Pankhurst *et al.* (2003) it is known that crystalline rocks of Cambrian age are buried 3,000-4,000 m below the Mesozoic to Cenozoic sedimentary infill of the Magallanes Basin. However, both these studies referred to samples from the same borehole (Gaviota Norte 6, Fig.1), therefore the areal extent of the Early Cambrian rocks remained uncertain.

In this paper, we present 5 new SHRIMP U-Th-Pb age determinations for zircons separated from gneisses and foliated intrusive rocks from the bottom of oil drill-holes in the Magallanes basin. These data, together with the previously published (Söllner *et al.*, 2000; Pankhurst *et al.*, 2003) and the two recently published (Hervé *et al.*, 2010) U-Pb ages of TFIMC magmatic zircons, and a petrographic study of a larger number of samples of similar source, are discussed and interpreted to provide a better understanding of the Paleozoic geological development of this portion of the Gondwana supercontinent.

2. Geological setting

Known occurrences of crystalline basement rocks in southern South America include the Sierra de la Ventana Fold Belt (Rapela *et al.*, 2003), the North Patagonian Massif, the Deseado Massif further to the southeast (Pankhurst *et al.*, 2003), and the rocks underlying the sedimentary successions of the Magallanes Basin in Tierra del Fuego (Söllner *et al.*, 2000; Pankhurst *et al.*, 2003).

According to recent paleotectonic reconstructions (Pankhurst *et al.*, 2006), the continental crust of part of this area is considered to have drifted away from Gondwana during the Early Cambrian in order to form an independent parautochthonous terrane (southern

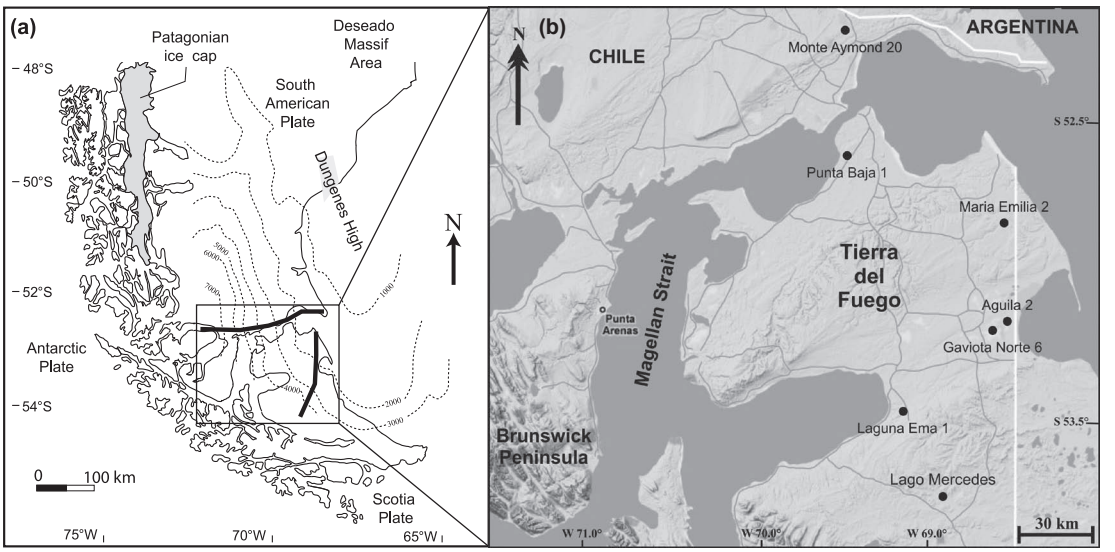

FIG. 1. Map of Tierra del Fuego and surroundings (a), showing the locations of the oil wells from which the samples analysed in this paper were taken (b). Thick solid lines in the inset (a) indicate the sections shown in figure 8. Dashed lines are depth contours (in meters) that delineate the top of the Jurassic volcanic rocks (Tobífera Formation; from Biddle *et al*., 1986).

Patagonia). This crustal block later collided during the mid-Carboniferous with the North Patagonian Massif, which was already forming part of Gondwana. Before the later break-up of Gondwana, southernmost Patagonia was probably continuous with part of East Antarctica and South Africa. The Weddell Sea and South Atlantic started to open in the Late Jurassic as a consequence of Gondwana break-up and a number of different models have been developed for the early opening of the Weddell Sea and the tectonic evolution of its neighbouring continents (*e.g.,* Suárez, 1976; LaBrecque and Barker,1981; Lawver *et al*., 1992; LaBrecque and Ghidella, 1997; Ghidella *et al*., 2002; König and Jokat, 2006). Southern Patagonian basement rocks formed during the Latest Proterozoic-Earliest Paleozoic are the result of the initial stages of formation of the Terra Australis orogen (Cawood, 2005) which evolved until the Late Paleozoic along the Pacific margin of Gondwana. Rocks of similar age are also found in the metamorphic basement of northwestern Argentina (*e.g.,* Ramos, 1988) and in the Deseado Massif in northern Patagonia (Pankhurst *et al.,* 2003). They are the result of continental margin orogenic events known as Pampean in Argentina, which can be broadly correlated with the Ross-Delamerian orogenies in East Antarctica and Australia (Transantarctic Mountains, Adelaide Fold Belt) (Söllner *et al.,* 2000).

3. Sample description

Samples for this study were obtained from the lowest parts of drill cores generated during Empresa Nacional del Petróleo (ENAP, Chile) hydrocarbon exploration activities in the Magallanes basin. Five samples were selected for U-Pb dating following microscopic examination of approximately 30 thin sections of the cores. The samples are geographically distributed in a roughly N-S stretching band, 50 km wide and 200 km long, west of the international border between Chile and Argentina (Fig.1b).

3.1. Águila 2 borehole, sample A2 518 M4-Augen gneiss

This rock is predominately composed by coarse-grained aggregates of quartz, plagioclase and K-feldspar, separated by finer bands of deformed and partly chloritized green biotite. The K-feldspar crystals also show microfaults. Interstitial carbonate partly replaces plagioclase. Zircon crystals are abundant, apatite and opaque minerals are accessory. In the same core, 30 cm long sections of peraluminous granitic gneisses with quartz, plagioclase, biotite and cordierite are present, as well as faintly foliated orthogneiss.

3.2. Gaviota Norte 6 borehole, sample GN6 2273 M1-Banded biotite orthogneiss

The sample consists of aggregates of quartz, plagioclase and biotite, the latter oriented and tending to form separate bands. Plagioclase is partially altered to calcite and chlorite, the biotite is mainly chloritized and altered peripherally to white mica. Opaque minerals are abundant. Euhedral zircon and apatite are common in the biotite bands. Microcataclastic bands cross-cut the rock.

3.3. María Emilia 2 borehole, sample ME2 1619 M2-Breccia of banded gneiss

The rock has a fragmental texture. All the angular fragments, up to 4 cm long, consist of quartzo-feldspathic gneiss, composed of quartz-plagioclase-K feldspar bands alternating with finer biotite-rich bands. Quartz crystals show only slight undulose extinction. The fine grained matrix between the clasts is not foliated; it contains small, undeformed biotite crystals, some of which bear fusiform prehnite inclusions. Titanite is abundant. The rock resembles a monomict sedimentary breccia rather than a tectonic breccia.

3.4. Monte Aymond 20 borehole, sample MA20 1011 M2-Migmatitic granitoid

This is a mixed rock, which has granitic and schistose portions. The peraluminous unfoliated granitic component consists of quartz, plagioclase, K-feldspar, and biotite in aggregates and bands which bear residual garnet with curved crystal limits and pinnitized cordierite megacrysts. The biotite bands are rich in zircon embedded in the biotite crystals. A similar rock type, without cordierite, consisting of quartz, plagioclase and orthoclase bands alternating with biotite-rich, sillimanite- and garnet-bearing ones, occurs in the core drilled at Laguna Ema 1, which has not been dated in this study.

3.5. Punta Baja 1 borehole, sample PB1 137 M2-Cordierite-sillimanite-garnet gneiss

In hand specimens, the rock shows 1-2 cm thick biotite rich (melanosome) and quartzo-feldespathic (leucosome) bands in similar proportions. A coarse-grained aggregate of quartz and partially chloritized biotite with oriented opaque mineral inclusions is predominant in the studied thin section. Cordierite is abundant and has inclusions of garnet with irregular curved shapes and fibrolite aggregates. Cordierite is partially transformed to pinnite. Zircon crystals included in the cordierite have opaque linings developing in their peripheries and cleavage cracks. Rutile is present in rather large crystal aggregates.

Additionally, comparison is made with SHRIMP U-Pb zircon ages of two samples from Lago Mercedes (samples LM1 and LM2; Hervé *et al.*, in press; Fig.1b): a foliated amphibolite and a banded orthogneiss.

The rocks of the TFIMC are mainly peraluminous cordierite granites, with variable tectonic transformation into orthogneisses, some with garnet, cordierite and sillimanite. The latter association is, in general, characteristic of rather low pressure metamorphism in the higher-temperature amphibolite facies, probably beyond the stability of white mica, which is conspicuously absent. Metaluminous hornblende-bearing granitoids are scarce and in our petrographic database restricted to the Lago Mercedes area (Fig.1b).

4. Methodology

The SHRIMP U-Pb ages were obtained on zircon concentrates prepared in the Departamento de Geología, Universidad de Chile, using SHRIMP II or SHRIMP RG at the Research School of Earth Sciences, The Australian National University, Canberra. The measurement techniques are similar to those described by Williams (1998, and references therein). Cathodoluminescence (CL) images were first obtained on all the sectioned zircon grains and used to target specific areas for analysis within the grains. The Temora reference zircon (Black *et al.*, 2003) was used to calibrate the U-Pb ratios, and the data were processed using the SQUID Excel macro of Ludwig (2001), plots and age calculations made using ISOPLOT (Ludwig, 2003). Tera-Wasserburg and relative probability diagrams for new crystallization ages of igneous rocks are shown in figure 2, and those for more complex samples in figure 3. CL images of five samples are shown in figures 4 and 5. The geological time-scale used is that of IUGS-ICS (http://www.stratigraphy.org).

Mineral phases of sample PB1 137 M1 were analysed on a CAMEBAX microprobe using a wavelength-dispersive spectrometer at the University of Montpellier, France. The standard operating

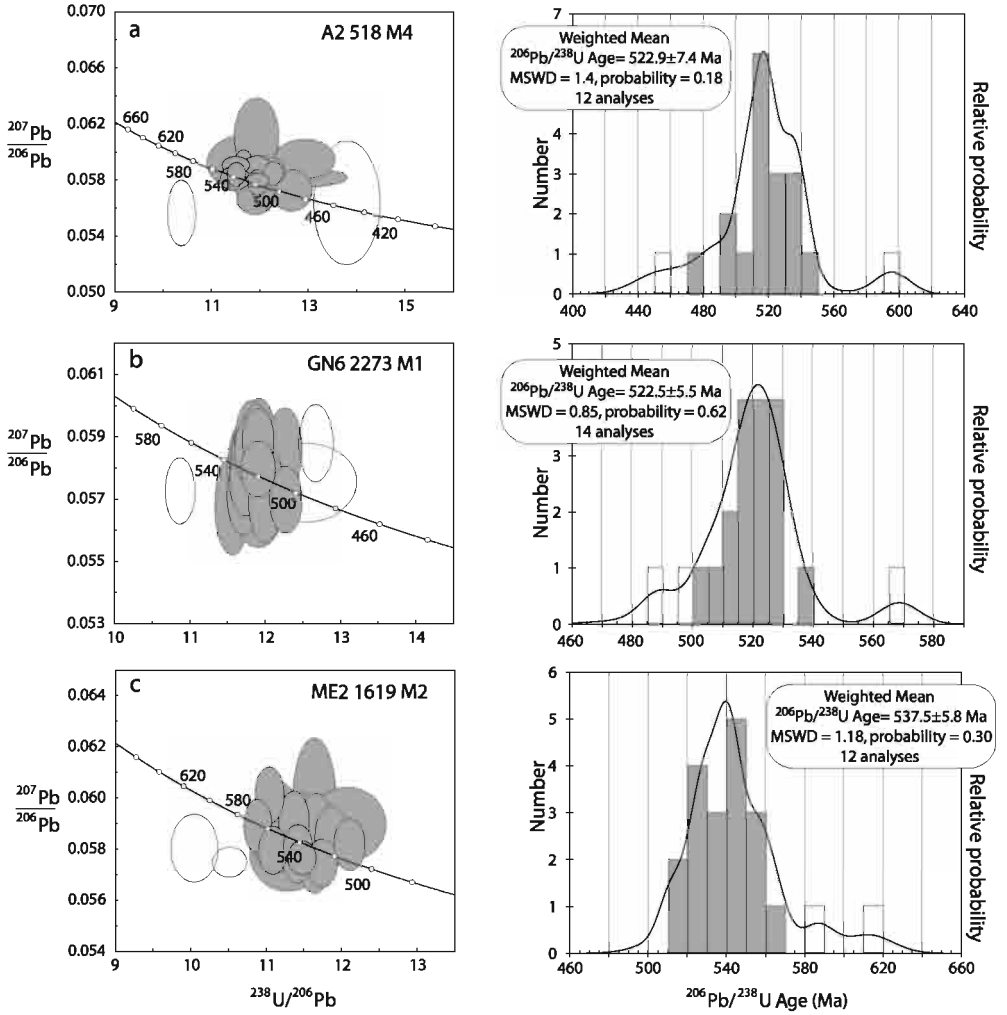

FIG. 2. Tera-Wasserburg and Relative Probability diagrams for the samples that yield Cambrian igneous crystallization age.

conditions included an accelerating voltage of 15 kV, a beam current of 10 nA, electron beam of 10-5 μm diameter and counting times ranging from 20 to 30 seconds depending on the element being analysed.

5. Previous age determinations

There have been a number of attempts to constrain the ages of basement rocks in the Magallanes basin. Halpern (1973) published a whole-rock Rb-Sr errorchron of 306±150 Ma (7 samples), and biotite mineral ages of 254±10 Ma (Rb-Sr) and 251±12 Ma (K-Ar) from gneissic granodiorite drill core samples. Unpublished radiometric age data is also available for basement samples obtained from the bottom of drill holes in the Magallanes Basin (Table 1). Internal ENAP reports (F. Escobar, 2006, written communication) indicate that eight K-Ar biotite ages range between 231 and 266 Ma. In addition, a Rb-Sr isochron of 267±3 Ma based on two whole rocks, plagioclase -biotite, and whole-rock isochrons of 324±64 Ma and 649±62 Ma are reported. A Jurassic Rb-Sr whole rock-biotite isochron age of 155±20 Ma in granodiorite and a K-Ar biotite age 185±5 Ma have been obtained and also given in this unpublished report. The interpretation of these ages will be made clear below, as no interpretation was provided for them in the written communication consulted.

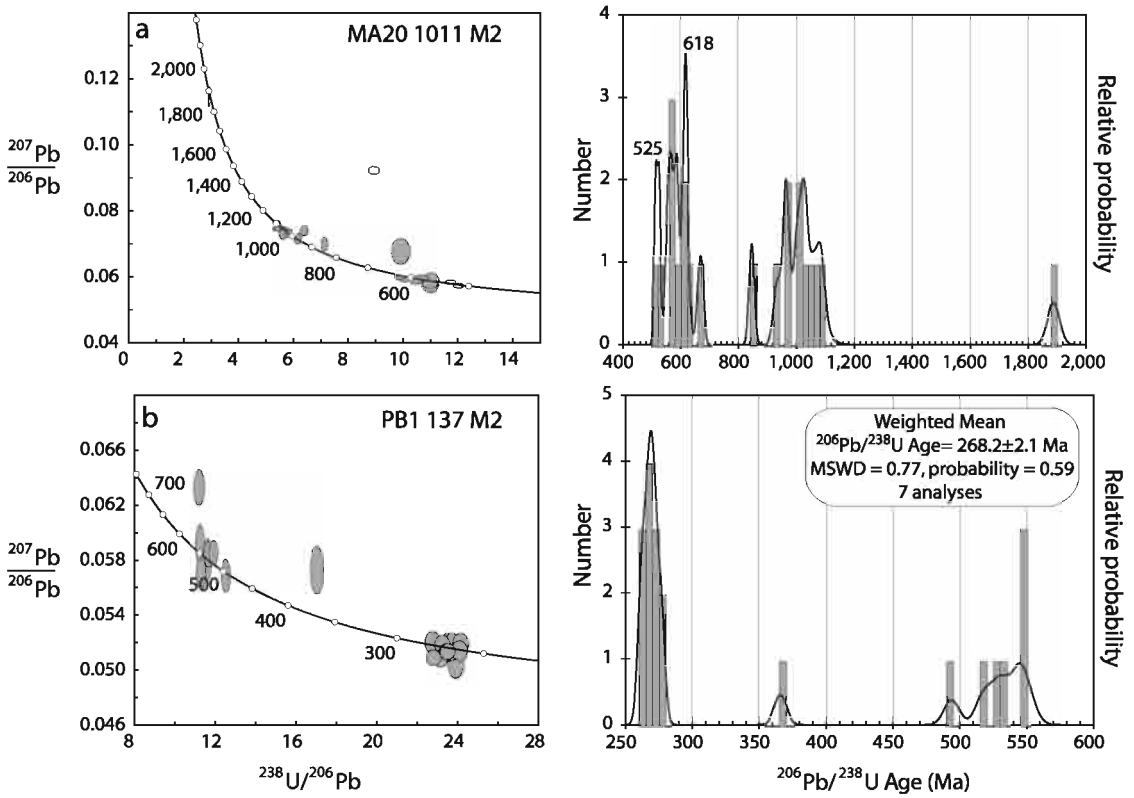

FIG. 3. Tera-Wasserburg and Relative Probability diagrams for the patterns of two of the gneisses which have an extended zircon age pattern.

TABLE 1. PREVIOUS K-Ar AGES OF MINERALS FROM ROCKS OF THE BOTTOM OF OIL WELLS IN THE MAGALLANES BASIN.

Sample	Well	Age±2σ (Ma)	Mineral	Rock
MGA T22 *	Gaviota Norte 6	261±6	biotite	Foliated quartz-biotite diorite
E-1 **	María Emilia 2	231±5	biotite	Gneissic granite
E-5 **	María Emilia 2	246±6	biotite	Gneissic granite
MA 2 ***	Monte Aymond 20	266±6	sericitic biotite	Biotite gneiss
DU 1 ****	Dungeness	261±6	biotite	Migmatitic gneiss
L M 1 ****	Lago Mercedes	247±8	biotite	Tonalite
L M 1 ****	Lago Mercedes	247±12	hornblende	Tonalite
****	María Emilia 2	251±12	biotite	Granodiorite gneiss

* Söllner *et al.* (2000); **Puig, A. (1984)[1]; ***Pérez de Arce, C. and Hervé, M. (1992)[2]; ****Moraga, J. (1994)[3].

The first U-Pb zircon analyses are given in Söllner *et al.* (2000). A granodiorite gneiss from the Gaviota Norte 6 borehole (Fig.1b) has zoned igneous zircons that yield a range of discordant $^{206}Pb/^{238}U$ ages. A concordia upper intercept age of 529±7.5 Ma was calculated for a series of unabraided grains, the abraded central portions of other grains giving a yet older upper intercept date of 549±6 Ma. The

[1] Puig, A. 1984. Empresa Nacional del Petróleo, internal report (unpublished).

[2] Pérez de Arce, C.; Hervé, M. 1992. Empresa Nacional del Petróleo, internal report (unpublished).

[3] Moraga, J. 1994. Empresa Nacional del Petróleo, internal report (unpublished).

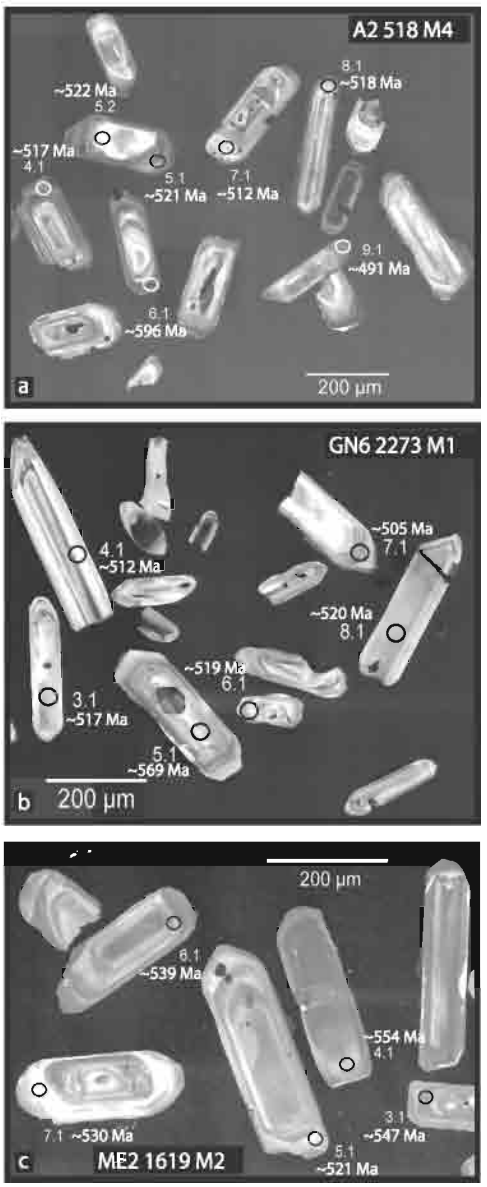

FIG. 4. Cathodoluminescence (CL) images of zircons considered to indicate igneous crystallization of the host rocks **a.** augen gneiss A2 518 M4; **b.** banded biotite orthogneiss GN6 2273 M1 and **c.** banded gneiss breccia ME2 1619 M2.

whole-grain upper intercept of 529±7.5 Ma was interpreted as the time of intrusion. Additionally, Söllner *et al.* (2000) report a K-Ar age of 261±6 Ma on biotite from the gneiss. A Rb-Sr two-point isochron on apatite and K-feldspar from the same rock gave 161.6±4.5 Ma, considered to relate to the Jurassic tectonomagmatic event in the area. They

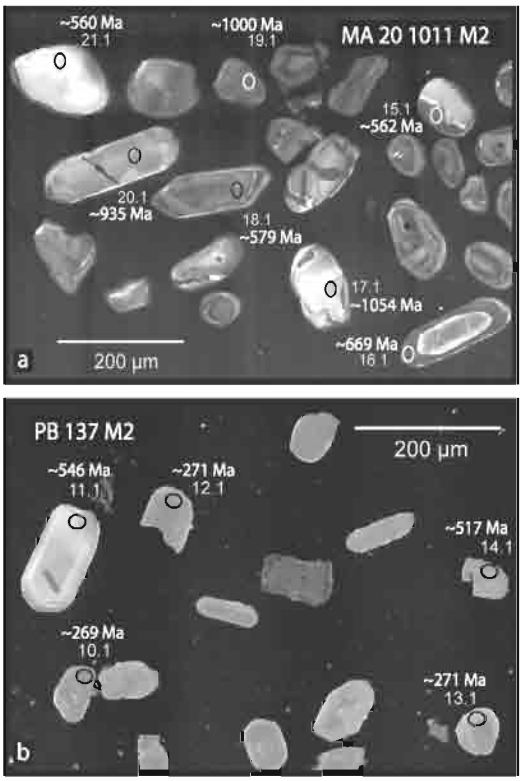

FIG. 5. Cathodoluminescence (CL) images of zircons from samples which have more complex zircon populations **a.** migmatitic granitoid MA20 1011 M2 and **b.** biotite-cordierite-sillimanite-garnet gneiss PB1 137 M2.

also obtained K-Ar ages of 171±9 Ma for hornblende from a dacite and 158±5 Ma for a whole rock basalt from the same drill core, both rocks belonging to the Tobífera Formation. Pankhurst *et al.* (2003) obtained a SHRIMP U-Pb zircon age of 523±5 Ma for a separate sampling of the same Gaviota 6 borehole orthogneiss. This age is for the euhedral tips and outer zones of sectioned zircon grains.

6. Results

A summary of the geochronological results obtained in this work is shown in table 2, with the full analytical data set in tables 3 to 7. The Aguila 2 borehole augen-gneiss has elongate, euhedral zircon grains, many with bipyramidal terminations, and simple oscillatory zoned interiors under CL imaging. Some grains are subround, interpreted as a consequence of the gneiss forming event. The $^{206}Pb/^{238}U$ ages form a dominant, slightly bimodal peak at about 525 Ma with tails on both younger

and older sides (Fig. 2a). There is one significantly older grain that likely reflects an inherited component (grain 7, ~596 Ma), whilst the younger analyses are interpreted to result from radiogenic Pb loss during the metamorphic overprint. A weighted mean of 12 analyses gives 523±7 Ma (MSWD=1.4) and this is considered to date the time of crystallisation of the dominant, zoned igneous zircon.

The Gaviota Norte 6 banded biotite orthogneiss also has elongate, euhedral zircon grains with bipyramidal terminations, although subround grains are more evident than in the Águila 2 sample. The CL images show a simple oscillatory zoned internal structure in elongated crystals with bipyramidal terminations. The data show a dominant age peak on the relative probability plot (Fig. 2b) although once again there is a single older analysis (grain 5, ~570 Ma) and a younger tail interpreted to arise from radiogenic Pb loss during the metamorphic overprint. The weighted mean age of 522.5±5.5 Ma (MSWD=0.85) is the time of zoned igneous zircon crystallisation.

The María Emilia 2 borehole breccia of biotite gneiss fragments yielded a notably homogeneous population of elongate euhedral zircon grains with bipyramidal terminations. The CL images show mostly simple oscillatory zoning, though some grains have central discontinuities which likely indicate the presence of older zircon components. The data for this sample form an asymmetric major age peak with two clearly older analyses (Fig. 2c). The data in the main peak is somewhat dispersed, but if the older (inherited components) and two younger (Pb loss) analyses are excluded the weighted mean for the remaining 13 gives 536±6 Ma (MSWD=1.6). Once again, this constrains the time of zoned igneous zircon crystallization, but there is evidence for inherited zircon and radiogenic Pb loss during the metamorphic overprint, though no new zircon formed.

Samples from the two other localities yielded even more complex results and this is commensurate with the zircon populations. The migmatitic granitoid from the Monte Aymond 20 borehole (Fig. 3a) has a wide range of zircon morphologies, from elongate euhedral grains with pyramidal terminations to round and subround, equant to elongate grains. The CL images highlight the complex nature of these zircon grains; many have darker more homogeneous areas that rim either zoned or other homogeneous metamorphic zircon cores. The metamorphic rims are of variable thickness, in some grains the zoned igneous core predominates. The U-Pb data is equally complex, for example the well developed metamorphic rims to grains 15 and 16 were analysed in the expectation that they would record a single event. However, grain 15 is latest Neoproterozoic ~560 Ma whereas grain 16 is 'Grenville' in age ~1,090 Ma. Overall, there is no uniform pattern of CL structure and age. The main age peaks span 550-650 Ma and 950-1,100 Ma, with a single grain giving ~1,900 Ma and so this sample appears to be a migmatite granite derived in part from the anatexis of metasediments with 'Grenville' and 'Brasiliano' provenance (and older), with a maximum age of 515-525 Ma as determined by the youngest two zircons dated.

The biotite-bearing cordierite-sillimanite-garnet gneiss from the Punta Baja 1 borehole (Fig. 3b) has a unique zircon population amongst this series of samples. The grains are notably smaller, most less than 100 μm in length, many less than 50 μm, and the grains are generally subhedral to subround. The CL images are consistently homogeneous grey in color, usually interpreted as indicating a metamorphic origin for the zircon. There are some grains

TABLE 2. NEW SHRIMP U-Pb AGE DETERMINATIONS IN SAMPLES OF THE BASEMENT ROCKS FROM THE BOTTOM OIL WELLS OF THE MAGALLANES BASIN.

Sample	Age (Ma)	Lithology	
A2 518 M4	522.9±7.4	Augen gneiss	Magmatic crystallization age
GN6 2273 M1	521.7±5.6	Banded biotite orthogneiss	Magmatic crystallization age
ME2 1619 M2	537.5±5.8	Breccia of banded gneiss	Magmatic crystallization age
MA20 1011 M2	Peaks at ranges ~1,090 and ~560	Migmatitic granitoid	Cambrian migmatization of Grenville age rocks
PB1 137 M2	Peaks at 268.2±2.6 and ~500 to ~550	Cordierite-sillimanite-garnet gneiss	Permian metamorphic event

TABLE 3. SUMMARY OF SHRIMP U-Pb RESULTS FOR ZIRCON FROM SAMPLE A2 518 M4 (AUGEN GNEISS).

Grain.	U	Th	Th/U	$^{206}Pb^*$	$^{204}Pb/$	f_{206}	Total				Radiogenic		Age (Ma)	
							$^{238}U/$		$^{207}Pb/$		$^{206}Pb/$		$^{206}Pb/$	
spot	(ppm)	(ppm)		(ppm)	^{206}Pb	%	^{206}Pb	±	^{206}Pb	±	^{238}U	±	^{238}U	±
1.1	322	92	0.29	24.2	0.000015	<0.01	11.407	0.145	0.0580	0.0005	0.0877	0.0011	542	7
2.1	77	37	0.48	5.7	0.000293	0.05	11.661	0.157	0.0584	0.0011	0.0857	0.0012	530	7
3.1	314	154	0.49	23.4	-	0.02	11.516	0.126	0.0584	0.0005	0.0868	0.0010	537	6
4.1	387	148	0.38	27.8	-	0.16	11.955	0.189	0.0590	0.0005	0.0835	0.0013	517	8
5.1	420	156	0.37	30.3	0.000028	<0.01	11.901	0.249	0.0566	0.0007	0.0841	0.0018	521	11
5.2	86	40	0.47	6.2	0.000198	<0.01	11.867	0.227	0.0578	0.0011	0.0843	0.0016	522	10
6.1	270	109	0.40	22.4	-	<0.01	10.381	0.190	0.0556	0.0016	0.0968	0.0018	596	11
7.1	146	69	0.47	10.3	0.000120	0.13	12.092	0.276	0.0586	0.0007	0.0826	0.0019	512	11
8.1	225	106	0.47	16.2	0.000055	0.01	11.958	0.132	0.0578	0.0006	0.0836	0.0009	518	6
9.1	376	161	0.43	25.6	0.000028	0.15	12.630	0.774	0.0582	0.0005	0.0791	0.0049	491	29
10.1	185	58	0.31	12.5	0.000064	0.03	12.648	0.282	0.0572	0.0010	0.0790	0.0018	490	11
11.1	373	130	0.35	26.1	-	0.14	12.270	0.132	0.0584	0.0006	0.0814	0.0009	504	5
12.1	164	60	0.37	10.9	0.000020	0.34	12.919	0.409	0.0595	0.0009	0.0771	0.0025	479	15
13.1	335	143	0.43	24.6	-	0.16	11.717	0.533	0.0592	0.0013	0.0852	0.0039	527	23
14.1	544	47	0.09	39.2	0.000073	0.43	11.927	0.304	0.0612	0.0018	0.0835	0.0022	517	13
15.1	755	79	0.10	47.0	0.000043	0.04	13.792	0.450	0.0563	0.0029	0.0725	0.0024	451	14
16.1	524	271	0.52	39.2	0.000032	0.10	11.504	0.188	0.0590	0.0004	0.0868	0.0014	537	9
17.1	789	299	0.38	56.7	-	0.04	11.956	0.154	0.0580	0.0003	0.0836	0.0011	518	7
18.1	217	106	0.49	15.4	0.000051	<0.01	12.073	0.156	0.0573	0.0008	0.0828	0.0011	513	6

Notes: **Calculated age considering the standard: 522.9±7.4 Ma**

1. Uncertainties given at the one σ level.
2. Error in Temora reference zircon calibration was 0.85% for the analytical session (not included in above errors but required when comparing data from different mounts).
3. f_{206} % denotes the percentage of ^{206}Pb that is common Pb.
4. Correction for common Pb for the U/Pb data has been made using the measured $^{238}U/^{206}Pb$ and $^{207}Pb/^{206}Pb$ ratios as outlined in Williams (1998).

TABLE 4. SUMMARY OF SHRIMP U-Pb RESULTS FOR ZIRCON FROM SAMPLE GN6 2273 M1 (BANDED BIOTITE ORTHOGNEISS).

							Total				Radiogenic		Age (Ma)	
Grain. spot	U (ppm)	Th (ppm)	Th/U	$^{206}Pb^*$ (ppm)	$^{204}Pb/^{206}Pb$	f_{206} %	$^{238}U/^{206}Pb$	±	$^{207}Pb/^{206}Pb$	±	$^{206}Pb/^{238}U$	±	$^{206}Pb/^{238}U$	±
1.1	241	144	0.60	17.2	-	<0.01	12.041	0.137	0.0574	0.0008	0.0831	0.0010	514	6
2.1	101	52	0.52	7.4	0.000323	0.01	11.754	0.152	0.0580	0.0010	0.0851	0.0011	526	7
3.1	160	97	0.61	11.5	-	<0.01	11.997	0.142	0.0568	0.0008	0.0834	0.0010	517	6
4.1	133	114	0.86	9.5	0.000189	0.04	12.104	0.221	0.0578	0.0009	0.0826	0.0015	512	9
5.1	192	151	0.79	15.2	-	<0.01	10.869	0.128	0.0572	0.0007	0.0922	0.0011	569	7
6.1	94	54	0.57	6.8	0.000345	0.11	11.919	0.153	0.0586	0.0011	0.0838	0.0011	519	7
7.1	150	99	0.66	10.5	0.000167	0.16	12.253	0.151	0.0586	0.0009	0.0815	0.0010	505	6
8.1	136	101	0.74	9.8	-	0.12	11.882	0.144	0.0588	0.0009	0.0841	0.0010	520	6
9.1	145	121	0.84	9.9	0.000095	0.05	12.518	0.460	0.0575	0.0008	0.0798	0.0030	495	18
10.1	163	92	0.56	11.0	-	0.23	12.672	0.149	0.0588	0.0008	0.0787	0.0009	489	6
11.1	132	103	0.78	9.5	0.000169	<0.01	11.906	0.215	0.0568	0.0009	0.0841	0.0015	521	9
12.1	153	89	0.59	11.2	0.000018	<0.01	11.704	0.138	0.0571	0.0008	0.0855	0.0010	529	6
13.1	149	91	0.61	10.9	0.000090	<0.01	11.734	0.139	0.0576	0.0008	0.0853	0.0010	527	6
14.1	79	54	0.69	5.9	0.000229	<0.01	11.558	0.153	0.0568	0.0010	0.0867	0.0012	536	7
15.1	113	77	0.68	8.2	-	0.11	11.808	0.147	0.0588	0.0009	0.0846	0.0011	523	6
16.1	90	44	0.50	6.6	-	<0.01	11.721	0.152	0.0579	0.0010	0.0853	0.0011	528	7
17.1	210	119	0.56	15.2	0.000080	0.14	11.908	0.139	0.0589	0.0007	0.0839	0.0010	519	6
18.1	198	113	0.57	13.9	-	<0.01	12.270	0.141	0.0570	0.0007	0.0815	0.0010	505	6
19.1	159	131	0.83	11.6	0.000184	0.08	11.795	0.134	0.0585	0.0007	0.0847	0.0010	524	6
20.1	234	155	0.66	16.9	-	0.03	11.906	0.152	0.0579	0.0006	0.0840	0.0011	520	6

Notes: **Calculated age considering the standard: 521.7±5.6 Ma**

1. Uncertainties given at the one σ level.
2. Error in Temora reference zircon calibration was 0.85% for the analytical session (not included in above errors but required when comparing data from different mounts).
3. f_{206} % denotes the percentage of ^{206}Pb that is common Pb.
4. Correction for common Pb for the U/Pb data has been made using the measured $^{238}U/^{206}Pb$ and $^{207}Pb/^{206}Pb$ ratios as outlined in Williams (1998).

TABLE 5. SUMMARY OF SHRIMP U-Pb RESULTS FOR ZIRCON FROM SAMPLE ME2 1619 M2 (BRECCIA OF BANDED GNEISS).

							Total				Radiogenic		Age (Ma)	
Grain. spot	U (ppm)	Th (ppm)	Th/U	$^{206}Pb^*$ (ppm)	$^{204}Pb/^{206}Pb$	f_{206} %	$^{238}U/^{206}Pb$	±	$^{207}Pb/^{206}Pb$	±	$^{206}Pb/^{238}U$	±	$^{206}Pb/^{238}U$	±
1.1	192	64	0.334	14.5	0.000089	0.09	11.38	0.13	0.0591	0.0008	0.0878	0.0011	542.5	6.3
2.1	364	216	0.594	27.4	-	<0.01	11.43	0.13	0.0581	0.0006	0.0875	0.0010	540.9	5.8
3.1	157	79	0.502	11.9	-	0.05	11.29	0.14	0.0588	0.0008	0.0885	0.0011	546.7	6.4
4.1	123	77	0.621	9.5	0.000111	0.03	11.13	0.22	0.0589	0.0012	0.0898	0.0018	554.3	10.9
5.1	214	100	0.465	15.5	-	0.09	11.88	0.14	0.0585	0.0008	0.0841	0.0010	520.7	6.2
6.1	675	106	0.157	50.5	0.000084	<0.01	11.48	0.12	0.0576	0.0004	0.0871	0.0009	538.6	5.6
7.1	50	24	0.483	3.7	0.000606	0.21	11.65	0.19	0.0598	0.0017	0.0857	0.0014	530.0	8.6
8.1	104	50	0.477	7.8	0.000082	0.03	11.48	0.21	0.0585	0.0011	0.0871	0.0016	538.1	9.5
9.1	368	155	0.420	26.9	0.000045	<0.01	11.75	0.13	0.0574	0.0006	0.0852	0.0010	526.9	5.9
10.1	199	99	0.496	14.6	-	0.12	11.67	0.14	0.0589	0.0008	0.0856	0.0010	529.3	6.1
11.1	148	88	0.595	12.7	0.000295	<0.01	10.05	0.21	0.0580	0.0009	0.0997	0.0021	612.8	12.2
12.1	165	117	0.713	12.1	0.000137	<0.01	11.65	0.15	0.0576	0.0008	0.0859	0.0011	531.4	6.5
13.1	223	98	0.441	17.3	0.000117	0.17	11.05	0.13	0.0601	0.0007	0.0903	0.0011	557.4	6.3
14.1	294	106	0.362	20.9	0.000048	0.08	12.11	0.14	0.0582	0.0007	0.0825	0.0009	510.9	5.6
15.1	289	113	0.391	22.3	0.000035	<0.01	11.10	0.12	0.0579	0.0006	0.0902	0.0010	556.7	6.1
16.1	126	73	0.585	8.9	0.000303	0.18	12.07	0.34	0.0590	0.0009	0.0827	0.0024	512.1	14.2
17.1	123	86	0.701	9.3	-	<0.01	11.29	0.33	0.0578	0.0010	0.0886	0.0026	547.5	15.5
18.1	160	79	0.493	12.1	0.000037	<0.01	11.41	0.14	0.0579	0.0008	0.0877	0.0011	541.7	6.4
19.1	228	77	0.338	17.9	-	<0.01	10.90	0.12	0.0589	0.0007	0.0918	0.0011	566.0	6.3
20.1	657	132	0.201	53.6	0.000038	-0.25	10.52	0.15	0.0575	0.0004	0.0953	0.0014	586.7	8.2

Notes: **Calculated age considering the standard: 537.5±5.8 Ma**

1. Uncertainties given at the one σ level.
2. Error in Temora reference zircon calibration was 0.59% for the analytical session (not included in above errors but required when comparing data from different mounts).
3. f_{206} % denotes the percentage of ^{206}Pb that is common Pb.
4. Correction for common Pb for the U/Pb data has been made using the measured $^{238}U/^{206}Pb$ and $^{207}Pb/^{206}Pb$ ratios as outlined in Williams (1998).

TABLE 6. SUMMARY OF SHRIMP U-Pb ZIRCON RESULTS FOR SAMPLE MA20 1011 M2 (MIGMATITIC GRANITOID).

					Total Ratios						Radiogenic Ratios							Age (Ma)				
Grain. spot	U (ppm)	Th (ppm)	Th/U	$^{206}Pb^*$ (ppm)	$^{204}Pb/^{206}Pb$	f_{206} %	$^{238}U/^{206}Pb$	±	$^{207}Pb/^{206}Pb$	±	$^{206}Pb/^{238}U$	±	$^{207}Pb/^{235}U$	±	$^{207}Pb/^{206}Pb$	±	ρ	$^{206}Pb/^{238}U$	±	$^{207}Pb/^{206}Pb$	±	% Disc
1.1	486	19	0.04	36	0.000127	0.13	11.748	0.127	0.0590	0.0005	0.0850	0.0009	-	-	-	-	-	526	6	-	-	-
2.1	281	87	0.31	34	0.000059	0.10	7.128	0.080	0.0706	0.0013	0.1402	0.0016	1.348	0.030	0.0697	0.0013	0.507	846	9	921	39	8
3.1	20	3	0.15	2	-	<0.01	9.917	0.219	0.0684	0.0026	0.1003	0.0023	0.892	0.057	0.0644	0.0035	0.550	616	13	756	116	18
4.1	323	88	0.27	28	0.000053	0.09	10.047	0.112	0.0600	0.0006	0.0998	0.0012	0.850	0.021	0.0618	0.0010	0.767	613	7	668	36	8
5.1	78	40	0.51	12	0.000140	0.24	5.448	0.074	0.0761	0.0010	0.1831	0.0025	1.870	0.046	0.0741	0.0015	0.552	1,084	14	1,044	41	-4
6.1	736	51	0.07	109	0.000001	0.00	5.774	0.061	0.0733	0.0005	0.1732	0.0018	1.749	0.021	0.0733	0.0005	0.861	1,030	10	1,021	13	-1
7.1	340	62	0.18	53	0.000044	0.08	5.526	0.188	0.0753	0.0005	0.1808	0.0061	1.863	0.065	0.0747	0.0007	0.969	1,072	34	1,060	18	-1
8.1	505	15	0.03	70	0.000008	0.01	6.209	0.067	0.0728	0.0008	0.1610	0.0017	1.614	0.024	0.0727	0.0008	0.709	963	10	1,005	22	4
9.1	513	4	0.01	37	0.000057	0.04	12.046	0.131	0.0579	0.0005	0.0830	0.0009	-	-	-	-	-	514	5	-	-	-
10.1	122	37	0.30	17	0.000081	0.14	6.159	0.077	0.0719	0.0008	0.1624	0.0021	1.620	0.043	0.0723	0.0013	0.770	970	12	995	38	3
11.1	424	114	0.27	37	0.000014	0.02	9.886	0.108	0.0605	0.0005	0.1011	0.0011	0.841	0.011	0.0603	0.0005	0.803	621	6	615	18	-1
12.1	247	116	0.47	20	0.000008	<0.01	10.452	0.140	0.0594	0.0007	0.0957	0.0013						589	8	-	-	-
13.1	1,037	330	0.32	152	0.000014	0.02	5.854	0.069	0.0748	0.0003	0.1708	0.0020	1.756	0.022	0.0746	0.0003	0.948	1,016	11	1,057	8	4
14.1	84	60	0.71	25	0.000069	0.11	2.937	0.037	0.1154	0.0021	0.3402	0.0043	5.369	0.121	0.1145	0.0021	0.560	1,887	21	1,872	34	-1
15.1	326	6	0.02	25	0.000036	<0.01	10.976	0.212	0.0585	0.0008	0.0911	0.0018	-	-	-	-	-	562	11	-	-	-
16.1	366	25	0.07	35	0.000000	<0.01	8.948	0.137	0.0929	0.0009	0.1094	0.0017	1.144	0.035	0.0759	0.0016	0.746	669	10	1,091	43	39
17.1	47	18	0.38	7	0.000070	0.12	5.625	0.088	0.0739	0.0013	0.1776	0.0028	1.784	0.048	0.0729	0.0016	0.581	1,054	15	1,011	45	-4
18.1	245	68	0.28	20	0.000089	0.12	10.633	0.203	0.0603	0.0007	0.0939	0.0018	-	-	-	-	-	579	11	-	-	-
19.1	393	169	0.43	57	0.000022	0.04	5.956	0.072	0.0732	0.0005	0.1678	0.0020	1.687	0.024	0.0729	0.0005	0.857	1,000	11	1,011	15	1
20.1	82	33	0.40	11	0.000088	0.15	6.396	0.102	0.0747	0.0010	0.1561	0.0025	1.580	0.035	0.0734	0.0012	0.712	935	14	1,025	32	9
21.1	29	36	1.22	2	0.000896	0.02	11.007	0.221	0.0589	0.0020	0.0908	0.0019	-	-	-	-	-	560	11	-	-	-

Notes:

1. Uncertainties given at the one σ level.
2. Error in Temora reference zircon calibration was 0.59% for the analytical session (not included in above errors but required when comparing $^{206}Pb/^{238}U$ data from different mounts).
3. f_{206} % denotes the percentage of ^{206}Pb that is common Pb.
4. For areas older than ~600 Ma correction for common Pb made using the measured $^{204}Pb/^{206}Pb$ ratio.
5. For areas younger than ~600 Ma correction for common Pb made using the measured $^{238}U/^{206}Pb$ and $^{207}Pb/^{206}Pb$ ratios as outlined in Williams (1998).
6. For % Disc, 0% denotes a concordant analysis.

TABLE 7. SUMMARY OF SHRIMP U-Pb RESULTS FOR ZIRCON FROM SAMPLE PB1 137 M2 (CORDIERITE-SILLIMANITE-GARNET GNEISS).

							Total				Radiogenic		Age (Ma)	
Grain. spot	U (ppm)	Th (ppm)	Th/U	$^{206}Pb^*$ (ppm)	$^{204}Pb/^{206}Pb$	f_{206} %	$^{238}U/^{206}Pb$	±	$^{207}Pb/^{206}Pb$	±	$^{206}Pb/^{238}U$	±	$^{206}Pb/^{238}U$	±
1.1	1237	6	0.005	45.9	0.000039	<0.01	23.15	0.24	0.0510	0.0004	0.0432	0.0005	272.8	2.8
2.1	396	2	0.005	14.5	0.000054	0.03	23.55	0.27	0.0518	0.0007	0.0424	0.0005	268.0	3.0
3.1	259	94	0.364	19.0	0.000084	0.08	11.71	0.15	0.0586	0.0006	0.0853	0.0011	527.8	6.7
4.1	596	3	0.004	21.2	-	0.07	24.18	0.26	0.0520	0.0006	0.0413	0.0005	261.1	2.8
5.1	1268	30	0.024	46.3	0.000043	<0.01	23.54	0.24	0.0515	0.0004	0.0425	0.0004	268.2	2.8
6.1	1045	14	0.013	52.7	-	0.45	17.05	0.22	0.0575	0.0012	0.0584	0.0008	365.8	4.7
7.1	1342	5	0.003	50.5	-	<0.01	22.83	0.24	0.0511	0.0004	0.0439	0.0005	276.7	2.8
8.1	670	4	0.006	25.3	0.000062	0.05	22.77	0.25	0.0522	0.0005	0.0439	0.0005	276.9	3.0
9.1	182	113	0.620	13.8	0.000158	<0.01	11.35	0.16	0.0572	0.0007	0.0882	0.0012	545.0	7.4
10.1	1124	10	0.009	41.1	0.000045	<0.01	23.49	0.24	0.0515	0.0004	0.0426	0.0004	268.8	2.8
11.1	133	73	0.547	10.1	0.000235	0.10	11.29	0.14	0.0593	0.0010	0.0884	0.0012	546.3	6.8
12.1	1164	4	0.003	43.0	0.000014	0.04	23.27	0.25	0.0520	0.0005	0.0430	0.0005	271.1	2.8
13.1	682	4	0.005	25.2	0.000074	<0.01	23.29	0.25	0.0514	0.0006	0.0430	0.0005	271.1	2.9
14.1	442	142	0.321	31.8	0.000148	0.13	11.96	0.13	0.0587	0.0006	0.0835	0.0010	517.1	5.7
15.1	988	4	0.004	35.2	0.000035	0.01	24.12	0.26	0.0516	0.0005	0.0415	0.0004	261.9	2.7
16.1	131	60	0.462	9.7	0.000152	0.03	11.64	0.15	0.0583	0.0010	0.0859	0.0011	531.0	6.7
17.1	466	2	0.005	16.7	0.000162	<0.01	23.93	0.27	0.0506	0.0007	0.0418	0.0005	264.2	2.9
18.1	550	2	0.004	19.9	0.000090	0.04	23.75	0.26	0.0519	0.0007	0.0421	0.0005	265.8	2.9
19.1	613	33	0.054	46.9	0.000040	0.62	11.24	0.17	0.0635	0.0009	0.0885	0.0014	546.4	8.2
20.1	295	104	0.354	20.2	0.000074	<0.01	12.56	0.15	0.0570	0.0008	0.0796	0.0009	494.0	5.7

Notes: **Calculated younger peak metamorphic age considering the standard: 268.2±2.6 Ma**

1. Uncertainties given at the one σ level.
2. Error in Temora reference zircon calibration was 0.59% for the analytical session (not included in above errors but required when comparing data from different mounts).
3. f_{206} % denotes the percentage of ^{206}Pb that is common Pb.
4. Correction for common Pb for the U/Pb data has been made using the measured $^{238}U/^{206}Pb$ and $^{207}Pb/^{206}Pb$ ratios as outlined in Williams (1998).

that have a faint zoning, which may be relict from an original igneous precursor. Due to the small size of the grains, it is not possible to analyze core or rim structures, and in most cases the grains are homogeneous. For the twenty grains analysed there is a predominant peak at about 260-270 Ma, the remaining eight $^{206}Pb/^{238}U$ ages are between ~495 and ~545 Ma, with an isolated grain at ~370 Ma. The metamorphic nature of the Permian-age zircon grains is highlighted by very low Th/U ratios (<0.02), the Cambrian grains having ratios between 0.3 and 0.62 as is normal for igneous zircon (Rubatto, 2002) (Fig. 6). A weighted mean for all 12 Permian grains has excess scatter (MSWD=3.3), but if the two oldest analyses are excluded the weighted mean is 267±3 Ma (MSWD=2.0). This metamorphic zircon probably formed during the episode that produced the garnet-sillimanite-cordierite assemblages, characteristic of upper amphibolite to granulite metamorphic facies (Vavra *et al.*, 1996).

According to P-T pseudo-sections calculated for this rock, Fe/(Fe+Mg) and Fe/(Fe+Mg+Ca+Mn) isopleths for biotite and garnet, respectively, in the corresponding mineral assemblage, metamorphic conditions can be restricted to the range 730-770°C and 2-3 kbar (Fig. 7). The calculated mineral assemblage at these conditions is the same as observed in the rock. The predicted proportions of biotite (*ca.* 4 vol.%) and cordierite (4 vol.%) appear to be smaller than in the studied rock. The calculated modal

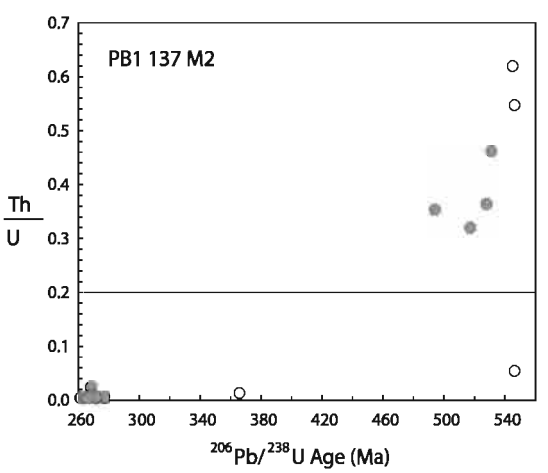

FIG. 6. Th/U *versus* age diagram for the zircon crystals from sample PB1 137 M2, in which the Permian metamorphic zircons differ completely from the older igneous ones.

mineralogy consists of approximately 30 vol.% of quartz, 12 vol.% of feldspars, 10 vol.% of sillimanite, 8 vol.% of garnet and 30 vol.% of haplogranitic melt. Anatexis and subsequent processes of melt (leucosome) migration through restitic material (melanosome) may explain the differences in modal mineralogy. Cordierite growth at expenses of biotite and garnet suggests that maximum metamorphic temperature was attained after the partial or complete disappearance of biotite.

The Lago Mercedes amphibolite and orthogneiss have also yielded Cambrian crystallization ages, similar to those obtained during this work (Hervé *et al.*, in press).

7. Interpretation

7.1. General

The Mesozoic-Cenozoic successions of the Magallanes Basin in Tierra del Fuego and part of the adjacent continental areas to the north are underlain by a crystalline basement complex here called the Tierra del Fuego Igneous and Metamorphic Complex (TFIMC). This complex is dominated by foliated peraluminous biotite granitoids, some containing cordierite and garnet, variably transformed to orthogneisses, some of them with ocellar structure. The attitude of the foliation is difficult to determine, but is usually at high angles to the core length, suggesting that a low-dipping foliation is predominant (Fig. 8).

Some of the gneisses contain the mineral assemblage cordierite-sillimanite-garnet-biotite-plagioclase-orthoclase-quartz. Usually, complete alteration of the cordierite to pinnite is observed, as well as partial chloritization of biotite, and partial replacement of plagioclase by carbonates. Later brittle deformation of the rocks is expressed by undulose extinction in quartz, microfractures and microbreccias.

Without exception, the zircon age spectra of all samples have a Cambrian component. The samples from Águila 2, Gaviota Norte 6 and María Emilia 2 contain only igneous zircons of this age (Table 2). These three populations are considered to reflect crystallization ages of the igneous protolith of the gneisses, with the zircons being dominantly simple, oscillatory zoned igneous grains as documented by CL images. Sample María Emilia 2 is a breccia composed of angular gneiss fragments, the scarce

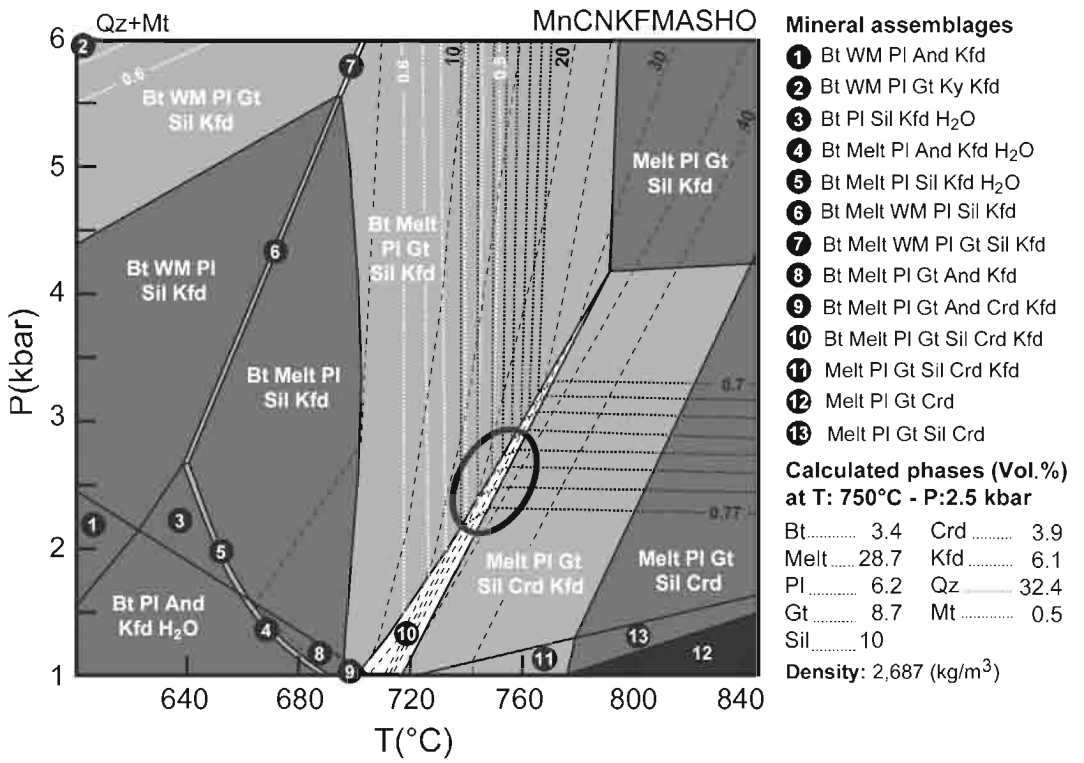

FIG. 7. Pressure-temperature pseudosection calculated for the biotite-cordierite-sillimanite-garnet gneiss (sample PB1 137 M1) at Punta Baja. Dashed white lines show the isopleths of the Fe/(Fe+Mg) ratio in biotite, ranging between 0.5 and 0.6 (see Table 8); dashed and black lines are the contour lines of the Fe/(Fe+Mg+Ca+Mn) ratio in garnet, ranging between 0.7 and 0.77. The dashed and thin black contour lines indicate the predicted volume % of melt in the PT compositional space. The mineral assemblage present in the rock, Fe/(Fe+Mg) and Fe/(Fe+Mg+Ca+Mn) isopleths of biotite and garnet, respectively, restrict the P-T metamorphic conditions to the range 730-770°C and 2-3 kbar (indicated by the ellipse). The calculated phases and their relative modal proportions at approximately 750°C and 2.5 kbar pressure conditions are indicated. The procedures for the P-T pseudosection calculation were as follows. The minimum free energy for an average bulk rock composition was calculated for a net of P-T conditions with the computer program package PERPLE_X (Connolly, 1990). Calculations were undertaken in the system MnO-Na_2O-CaO-K_2O-FeO-MgO- Al_2O_3-SiO_2-H_2O-O_2 for the P-T range 1-10 kbar and 600-1,000°C. The thermodynamic calculation excluded the TiO_2 component, which in the rock is mainly accommodated in biotite and rutile. We used the thermodynamic data set of Holland and Powell (1988, updated 2002) for mineral and aqueous fluid. The later solid-solution models (see Powell and Holland, 1999), being compatible with this data set, were selected from the downloaded version of the PERPLE_X solution-model file (newest_format_solut. dat): Bio(HP) for biotite, Pl(h) plagioclase, Gt(HP) for garnet, Pheng(HP) for potassic white mica, and melt(HP) for melt. K-feldspar was considered as a pure phase. Mineral abbreviations are: And, andalusite; Bt, biotite; Crd, cordierite; Gt, garnet; Kfd, K-feldspar; Ky, kyanite; Mt, magnetite; Pl, plagioclase; Qz, quartz; Sil, sillimanite; WM, white mica. The graphical results were taken as raw data. The final pseudosection was redrawn by smoothing curves as demonstrated by Connolly (2005). The major elements bulk chemical composition of rock sample PB1 137 M1 was determined with a PHILIPS PW 2400 X-ray fluorescence (XRF) spectrometer at Stuttgart University. The bulk rock composition (wt%) is SiO_2: 65.07, TiO_2: 0.81, Al_2O_3: 17.61, Fe_2O_3: 6.54, MgO: 1.59, MnO: 0.06, CaO: 0.50, Na_2O: 0.96, K_2O: 2.80 and P_2O_5: 0.12. The original rock composition was simplified to fit the used system (without TiO_2). An oxygen content of 0.065 wt% was selected corresponding to 10% Fe^{3+} of the total iron (see Massonne *et al.*, 2007) and a 1 wt% of water content was considered in the calculation.

intervening matrix has a sedimentary character rather than a cataclastic one. The breccia probably originated from sedimentary strata covering the gneissic basement and consists entirely of reworked basement fragments.

The migmatitic granite MA20 1011 M2 contains complex zircon grains and appears to be derived from a metasediment with 'Grenville' and 'Brasiliano' provenance, with a maximum protolith age of 515-525 Ma as determined by the youngest two zircons dated.

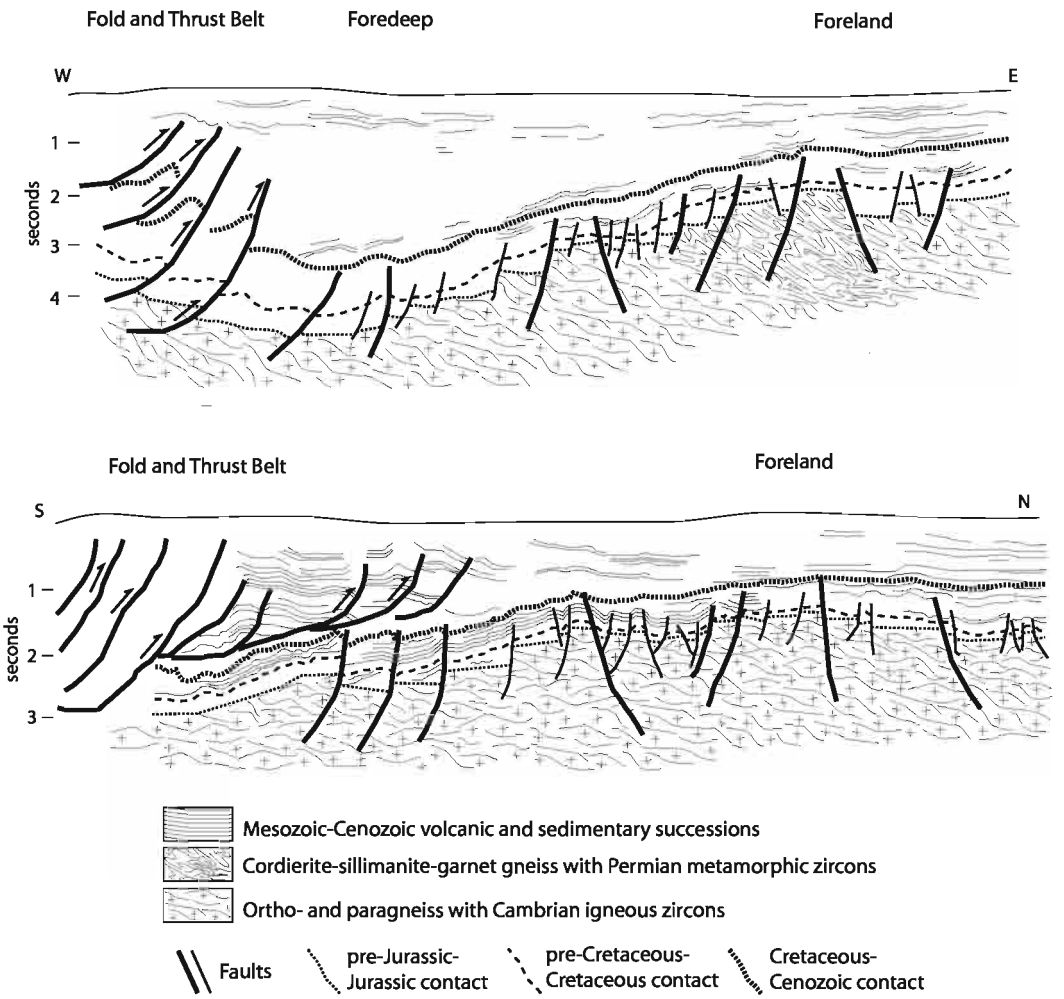

FIG. 8. Cross-sections of the Magallanes Basin, showing the east- and northward prograding thrust pile over the basin (Harambour, 1998); main structures and depositional contacts between Cretaceous and Cenozoic sequences are from seismic lines. The contact between pre-Jurassic and Jurassic (Tobífera) units is a rough approximation. Oil wells are located in the foreland basin area.

The cordierite-sillimanite-garnet gneiss PB1 137 M2 features a predominant Permian (267±3 Ma) peak of metamorphic zircons, with some older grains in the range ~495-545 Ma. This is interpreted as resulting from a high temperature Permian metamorphic event that affected either a Cambrian igneous protolith, probably similar to Águila 2 and Gaviota Norte 6 rocks dated here, or a sedimentary rock derived from Cambrian igneous rocks.

A Permian event is also indicated by the Rb-Sr (see text) and K-Ar biotite ages (Table 1) previously obtained from the basement rocks, but which were considered to be reset ages representing opening of the isotopic systems or cooling ages. They can now be interpreted as dating the closure of Rb-Sr and K-Ar systems during or after the Permian metamorphic event, which very probably formed the biotite in the dated gneiss, and probably also in the regional foliated granitoids. It is possible that all the gneisses studied here developed their foliation during this Permian metamorphism, but that only the rocks at the highest grades developed Permian zircon. The K-Ar dating of biotite crystals (~265 to 230 Ma) in the gneisses of the TFIMC, either newly formed or reset, or both, indicate cooling of the rocks after the Permian tectonometamorphic event.

TABLE 8. REPRESENTATIVE ELECTRON MICROPROBE ANALYSES OF MINERALS IN CORDIERITE-SILLIMANITE-GARNET GNEISS (SAMPLE PB1 137 M2).

Mineral -	Garnet					
Analysis No.	#47	#59	#60	#65	#70	#76
SiO_2	38.24	38.46	38.43	38.31	37.93	37.69
TiO_2	0.00	0.03	0.01	0.02	0.00	0.01
Al_2O_3	21.77	21.68	21.73	21.59	21.69	21.27
Cr_2O_3	0.03	0.02	0.01	0.00	0.01	0.02
FeO	32.62	33.20	32.34	33.56	34.61	33.67
Fe_2O_3	-	-	-	-	-	-
MnO	1.29	1.33	1.26	1.36	1.82	1.89
MgO	5.06	4.79	5.66	4.96	4.04	3.95
CaO	1.90	1.58	1.24	1.23	1.11	1.32
Na_2O	0.02	0.03	0.00	0.01	0.01	0.01
K_2O	-	-	-	-	-	-
H_2O	-	-	-	-	-	-
Total	100.93	101.12	100.68	101.03	101.22	99.84
Si	6.01	6.07	6.05	6.04	5.99	6.06
Al_t	-	-	-	-	-	-
Ti	0.00	0.00	0.00	0.00	0.00	0.00
Al_o	4.03	4.03	4.03	4.01	4.04	4.03
Cr	0.00	0.00	0.00	0.00	0.00	0.00
Fe_3	-	-	-	-	-	-
Fe_2	4.28	4.38	4.26	4.43	4.57	4.53
Mn	0.17	0.18	0.17	0.18	0.24	0.26
Mg	1.18	1.13	1.33	1.17	0.95	0.95
Ca	0.32	0.27	0.21	0.21	0.19	0.23
Na	0.01	0.01	0.00	0.00	0.00	0.00
K	-	-	-	-	-	-
H	-	-	-	-	-	-
Components						
grossular	0.05	0.04	0.03	0.03	0.03	0.04
pyrope	0.20	0.19	0.22	0.19	0.16	0.16
almandine	0.72	0.73	0.71	0.74	0.77	0.76
spessartine	0.03	0.03	0.03	0.03	0.04	0.04
xAl	1.00	1.00	1.00	1.00	1.00	1.00

Mineral -	Biotite				
Analysis No.	#48	#56	#61	#66	#77
SiO_2	35.37	34.85	35.94	34.45	35.00
TiO_2	3.54	5.64	4.92	3.51	5.25
Al_2O_3	17.89	17.55	17.49	17.26	17.40
Cr_2O_3	0.03	0.08	0.08	0.05	0.06
FeO	19.06	20.34	19.37	18.83	19.68
Fe_2O_3	-	-	-	-	-
MnO	0.06	0.06	0.05	0.02	0.05
MgO	10.15	7.36	8.59	10.13	9.24
CaO	0.01	0.00	0.03	0.01	0.12
Na_2O	0.14	0.12	0.15	0.11	0.18
K_2O	9.90	9.75	9.89	9.80	9.88
H_2O	3.96	3.92	3.97	3.87	3.97
Total	100.12	99.67	100.49	98.04	100.83
Si	2.68	2.67	2.71	2.67	2.64
Al_t	1.32	1.33	1.29	1.33	1.36
Ti	0.20	0.32	0.28	0.20	0.30
Al_o	0.27	0.25	0.27	0.25	0.19
Cr	0.00	0.00	0.00	0.00	0.00
Fe_3	-	-	-	-	-
Fe_2	1.21	1.30	1.22	1.22	1.24
Mn	0.00	0.00	0.00	0.00	0.00
Mg	1.15	0.84	0.97	1.17	1.04
Ca	0.00	0.00	0.00	0.00	0.01
Na	0.02	0.02	0.02	0.02	0.03
K	0.96	0.95	0.95	0.97	0.95
H	2.00	2.00	2.00	2.00	2.00
Component and ratio					
xAl	0.14	0.13	0.13	0.12	0.10
Fe/(Fe+Mg)	0.51	0.61	0.56	0.51	0.54

Mineral -	Plagioclase	
Analysis No.	#67	#68
SiO_2	61.20	61.04
TiO_2	0.00	0.01
Al_2O_3	24.54	24.71
Cr_2O_3	0.00	0.02
FeO	-	-
Fe_2O_3	0.06	0.04
Mn_2O_3	0.00	0.00
MgO	0.00	0.00
CaO	5.97	6.24
Na_2O	7.65	7.95
K_2O	0.35	0.34
H_2O	-	-
Total	99.78	100.37
Si	2.72	2.71
Al	1.29	1.29
Fe_3	0.00	0.00
Ti	0.00	0.00
Cr	0.00	0.00
Fe_3	-	-
Fe_2	-	-
Mn_3	0.00	0.00
Mg	-	-
Ca	0.28	0.30
Na	0.66	0.68
K	0.02	0.02
H	-	-
Components		
An	0.30	0.30
Ab	0.68	0.68
Or	0.02	0.02

Mineral -	K-feldspar		
Analysis No.	#51	#54	#58
SiO_2	63.97	64.33	64.44
TiO_2	0.00	0.01	0.00
Al_2O_3	18.88	18.65	18.91
Cr_2O_3	0.00	0.00	0.00
FeO	-	-	-
Fe_2O_3	0.00	0.04	0.03
Mn_2O_3	0.00	0.00	0.00
MgO	0.01	0.01	0.01
CaO	0.15	0.09	0.21
Na_2O	1.72	1.63	2.32
K_2O	14.60	14.87	13.74
H_2O	-	-	-
Total	99.32	99.63	99.66
Si	2.97	2.98	2.97
Al	1.03	1.02	1.03
Fe_3	0.00	0.00	0.00
Ti	0.00	0.00	0.00
Cr	0.00	0.00	0.00
Fe_3	-	-	-
Fe_2	-	-	-
Mn_3	0.00	0.00	0.00
Mg	-	-	-
Ca	0.01	0.00	0.01
Na	0.15	0.15	0.21
K	0.86	0.88	0.81
H	-	-	-
Components			
An	0.01	0.00	0.01
Ab	0.15	0.14	0.20
Or	0.84	0.85	0.79

Mineral -	Sillimanite			
Analysis No.	#49	#57	#73	#74
SiO_2	37.84	37.14	36.77	36.97
TiO_2	0.00	0.03	0.00	0.03
Al_2O_3	63.37	62.60	62.95	62.73
Cr_2O_3	0.03	0.01	0.01	0.03
FeO	-	-	-	-
Fe_2O_3	0.18	0.15	0.18	0.21
Mn_2O_3	0.01	0.01	0.00	0.00
MgO	-	-	-	-
CaO	0.01	0.01	0.00	0.00
Na_2O	0.01	0.00	0.00	0.00
K_2O	-	-	-	-
H_2O	-	-	-	-
Total	101.45	99.94	99.92	99.96
Si	1.01	1.00	0.99	1.00
Al	1.99	1.99	2.00	2.00
Fe_3	0.00	0.00	0.00	0.00
Ti	0.00	0.00	0.00	0.00
Cr	0.00	0.00	0.00	0.00
Fe_3	0.00	0.00	0.00	0.00
Fe_2	-	-	-	-
Mn_3	0.00	0.00	0.00	0.00
Mg	-	-	-	-
Ca	0.00	0.00	0.00	0.00
Na	0.00	0.00	0.00	0.00
K	-	-	-	-
H	-	-	-	-

Mineral -	Chlorite
Analysis No.	#52
SiO_2	27.58
TiO_2	3.05
Al_2O_3	17.47
Cr_2O_3	0.03
FeO	29.01
Fe_2O_3	-
MnO	0.20
MgO	10.20
CaO	-
Na_2O	-
K_2O	-
H_2O	11.16
Total	98.70
Si	5.93
Al_t	2.07
Al_o	2.35
Cr	0.00
Ti	0.49
Fe_3	-
Fe_2	5.21
Mn	0.04
Mg	3.27
Ca	-
Na	-
K	-
H	16.00
Compositions	
xSi	0.96
xMg	0.38
xFe	0.61

Mineral -	Cordierite (pinnitized)				
Analysis No.	#63	#69	#71	#72	#75
SiO_2	41.25	41.08	46.37	46.18	45.20
TiO_2	0.02	0.00	0.02	0.01	0.04
Al_2O_3	28.24	29.85	32.74	30.77	32.69
Cr_2O_3	0.00	-0.00	-0.00	0.03	0.01
FeO	10.04	9.95	6.93	6.75	7.32
Fe_2O_3	-	-	-	-	-
MnO	0.09	0.07	0.03	0.03	0.05
MgO	4.83	4.67	1.99	1.97	1.94
CaO	1.04	0.89	2.00	1.84	1.81
Na_2O	0.13	0.07	0.13	0.20	0.16
K_2O	0.61	0.93	1.27	0.95	0.88
H_2O	-	-	-	-	-
Total	86.24	87.52	91.48	88.72	90.10

Mineral -	Magnetite	
Analysis No.	#50	#53
SiO_2	0.12	0.15
TiO_2	0.01	0.00
Al_2O_3	0.00	0.01
Cr_2O_3	0.00	0.00
FeO	59.23	60.97
MnO	0.00	0.00
MgO	0.00	0.00
CaO	0.01	0.00
Na_2O	0.06	0.03
K_2O	0.00	0.01
NiO	0.48	0.01
Total	59.86	61.15

The TFIMC rocks experienced yet younger events that modified their isotopic composition. Söllner *et al.* (2000) obtained a Jurassic mineral isochron in the rock dated as Cambrian by U-Pb zircon, and another previous Rb-Sr age also recorded this Jurassic younger event in the granodiorite. These have been related to the magmatic event that occurred in the area during the Middle to Late Jurassic associated with extension during the initial stages of Gondwana break-up, which also generated the Tobífera Formation (Pankhurst *et al.*, 2000). Obviously this event did not result in the resetting of the U-Pb zircon ages, but may have locally modified less resistant isotopic systems.

7.2. Comparison with neighbouring areas in Patagonia and Malvinas/Falkland islands

The Cape Meredith complex in the Malvinas/ Falkland islands is composed of Mesoproterozoic basement gneisses and granitoids which have been compared in broad terms to the Namaqua-Natal-Dronning Maud Land metamorphic belt in southern Africa and Antarctica (Groenewald *et al.*, 1991). SHRIMP U-Pb zircon ages date the oldest felsic gneisses at 1,118±8 Ma and cross-cutting igneous phases at *ca.*, 1,090, 1,067±9 and 1,003±16 Ma (Jacobs *et al.*, 1999), similar to the inherited zircon ages obtained here from the sample from Monte Aymond 20 borehole.

No Cambrian plutonic rocks or (meta-) sedimentary rocks containing predominantly Cambrian zircons are known from the Deseado Massif (Pankhurst *et al.*, 2003) in Argentine Patagonia (Fig. 9), although Pezzuchi (1978) reported a 540±20 Ma K-Ar amphibole date for an amphibolite. However, the basement rocks of the Sierra de la Ventana succession, north of the Río Colorado, include Early Cambrian A- and I-type granites (Rapela *et al.*, 2003), of the same age as those studied here, and low-grade metasedimentary rocks in the eastern part of the North Patagonian Massif contain predominant Cambrian detrital zircons as their youngest component (Pankhurst *et al.*, 2006). The metasedimentary rocks of the Eastern Andes Metamorphic Complex exhibit varied detrital zircon age patterns (Hervé *et al.*, 2003; Augustsson and Bahlburg, 2007), most of them with prominent Cambrian components, but extending into the Silurian, Devonian, Carboniferous and Permian. The Cordillera Darwin Metamorphic Complex (Hervé *et al.*, in press) presents a significant number of detrital zircon age spectra and some of the samples include groups with Cambrian ages, as well as Silurian to Devonian components. The Duque de York Complex in the Madre de Dios archipelago, on the contrary, has prominent Permian but no Cambrian components. However, these zircons are igneous in origin (Sepúlveda *et al.*, this volume), and not metamorphic as we have observed and documented for the Punta Baja gneiss.

7.3. Comparison with the Antarctic Peninsula

In this context it is very important to consider also the evolution of the basement of the Ellsworth Mountains and of the Antarctic Peninsula, which, like Patagonia, represent fragments of the former southwestern Gondwana margin. Cambrian zircons are common in the Ellsworth Mountains metasedimentary succession (Flowerdew *et al.*, 2007), deposition of which spans the whole of the Paleozoic era. However, only minor outcrops of Late Cambrian igneous rocks are known (Vennum *et al.*, 1992). The early stages of this succession are thought to have been deposited in an active rift that later evolved to a passive margin. The basement to this succession is considered to be represented by the granitic gneisses and leucogranites that crop out on the isolated Haag Nunataks; these have yielded Rb-Sr whole-rock isochron ages of 1,176±76 Ma, 1,058±53 Ma and 1,008±18 Ma (Millar and Pankhurst, 1987), which may be considered as reasonably consistent with the dated events in the Cape Meredith complex. The sedimentary provenance may initially have been mainly from southernmost Africa, and later on from a more expansive source region within West Gondwana, probably including the Kaapvaal and Congo cratons of southern and western Africa.

In the Antarctic Peninsula, crystalline basement rocks comprising mainly granitic orthogneisses, migmatites and layered paragneisses, are exposed in small, isolated outcrops (Adie, 1962). The oldest of these rocks are paragneisses cropping out at Adie Inlet on the eastern coast of Graham Land (Fig. 9). They contain predominantly Cambrian zircons (18 grains at 520±8 Ma), but also some younger Paleozoic detrital grains, and experienced high-grade metamorphism and migmatization at 258±3 Ma (Millar *et al.*, 2002). The Permian zircons feature low Th/U ratios (<0.08) and differ significantly

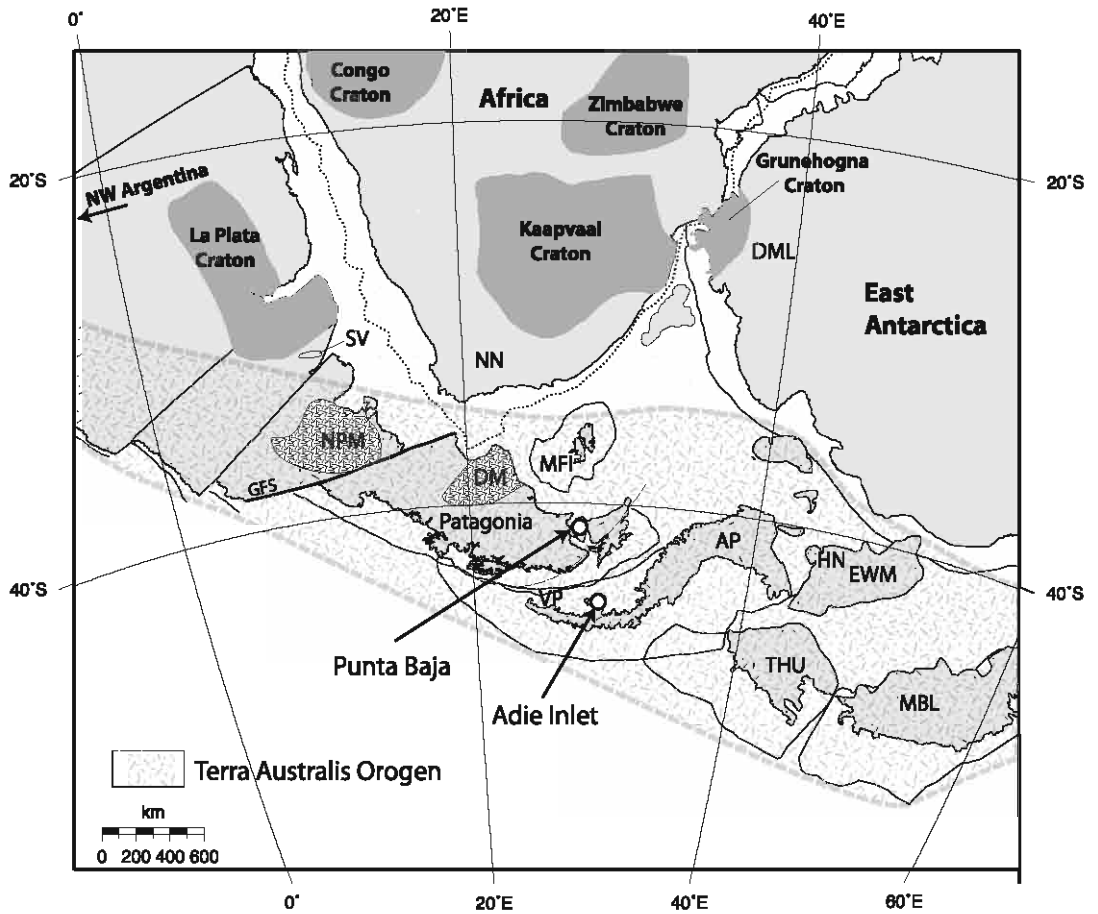

FIG. 9. Paleogeographic reconstruction modified from König and Jokat (2006) showing the main units mentioned in the text. Dark grey areas indicate cratons in the SW Gondwana assemblage. Paleolatitudes correspond to *ca.* 167 Ma. Limits of the Terra Australis Orogen taken from Cawood (2005). Abbreviations used in this figure are **AP:** Antarctic Peninsula; **DM:** Deseado Massif; **DML:** Dronning Maud Land; **EWM:** Ellsworth Whitmore Mountains; **GFS:** Gastre Fault System; **HN:** Haag Nunataks; **MFI:** Malvinas/Falkland Islands; **MBL:** Marie Byrd Land; **NN:** Namaqua-Natal Province; **NPM:** North Patagonian Massif; **THU:** Thurston Island; **SV:** Sierra de la Ventana; **VP:** View Point.

from the zoned Cambrian zircons which display Th/U ratios of 0.41-0.88. These observations are strikingly similar to those presented here for the Punta Baja 1 sample, and indicate similar and contemporaneous processes affecting both areas. Permian (and Triassic) granitoids crop out sporadically along the Antarctic Peninsula, and many of them are 'S-type' (Millar *et al.*, 2002).

The relative position of the Antarctic Peninsula is assumed to have been adjacent to and contiguous with Patagonia during the Early Mesozoic (König and Jokat, 2006; Hervé *et al.*, 2006) before Gondwana break-up. Such a paleogeographic configuration would locate Adie Inlet close to Tierra del Fuego.

7.4 Regional tectonics

Zircon ages of approximately1,000 Ma ('Grenvillian') are common along the paleo-Pacific margin of Gondwana, whereas Cambrian igneous and metamorphic rocks are common in NW Argentina (the Pampean orogen) and in parts of Eastern Antarctica (Ross orogen). This suggests that the rocks studied here could have formed part of a previously more extensive (continuous?) magmatic province along the Gondwana margin, as noted by Söllner *et al.* (2000). However, Rapela *et al.* (2001) considered the Pampean orogen, which includes peraluminous granites and high-T metamorphic rocks, as a spatially

restricted tectono-magmatic belt related to the collision of a Pampean micro-continent with the margin of a larger continent to the east, and in this context no continuity can be established with the Tierra del Fuego basement rocks.

A similar microcontinent collision has been advocated to explain the development of the Ross-Delamerian orogen rocks, including the collision of small terranes during subduction processes (Glen, 2005). If the peraluminous granitic rocks of the TFIMC were also produced by a continental collision, then involvement of another micro-continent would be necessary to explain this occurrence. Alternatively, Dalziel (1997) proposed a model in which the subduction-generated Pampean magmatic arc was related to the approach of a large craton, Laurentia, which would have collided with western South America in early Ordovician times.

Permian zircons of roughly the same age as those seen in the Punta Baja 1 sample (269 Ma) are common as detrital zircons in the Eastern Andes Metamorphic Complex and predominant in the Duque de York complex (Hervé *et al.*, 2006). However, most of those detrital zircons are typical igneous ones, whereas those studied here have metamorphic characteristics. This event is contemporaneous with widespread Permian intrusive activity in the North Patagonian Massif, which may have been initiated when the subducted slab broke off, following the collision between southern Patagonia and Gondwana (Pankhurst *et al.*, 2006). It is possible that a southward prolongation of the Permian magmatic belt, which at present crops out only from the North Patagonian Massif northwards, lies hidden beneath younger sedimentary and/or volcanic units located between the North Patagonian Massif and the Magallanes basin. Recently, Ramos (2008) suggested that a Carboniferous magmatic arc could be buried below the sedimentary rocks of the Magallanes basin forming the ridge known as the Dungeness High. The rocks studied here lie west of this arc, and have not yielded zircons of Carboniferous age. It might also be suggested that a hypothetical micro-continental mass (the Antarctic Peninsula?) collided with the continental margin of Gondwana during Late Paleozoic times, as part of the amalgamation of Pangea.

A special geological feature of the TFIMC is the absence of the Paleozoic sedimentary cover typical for Cambrian basement elsewhere in the region (Sierra de la Ventana, the Cape Fold Belt in South Africa, the Ellsworth-Whitmore mountain block and northern Victoria Land in Antarctica). The TFIMC level presently covered by the Jurassic Tobífera Formation was 8 to 12 km below the surface during the Permian tectonometamorphic event, as suggested by the 2-3 kbar pressure determined here, and was exhumed before the Middle Jurassic; it would thus have been an important source of Cambrian to Permian aged detritus to the surrounding areas. The Permian conglomerates of the La Golondrina Formation in extra-Andean Patagonia (Pankhurst *et al.*, 2003), in South Africa (Fildani *et al.*, 2009), in the Antarctic Peninsula (View Point, Millar *et al.*, 2002; Paradise Bay, Kraus 2007) and in the Duque de York Formation (Faúndez *et al.*, 2002) may be the result of this exhumation process which might have involved temperate glacial erosion processes in an orographic high.

Acknowledgements

The SHRIMP age determinations carried out at the Australian National University were financed by FONDECYT project 1050431 (FH) and MF research funds. This is also a contribution to FONDECYT projects 11075000 (MC) and 1095099 (FH), a CONICYT-BMBF project to Dr. H. Massonne (University of Stuttgart) and FH, and to Anillo Antártico Project ARTG-04 (CONICYT-World Bank). We thank Empresa Nacional del Petróleo (ENAP) geologists G. Romero and A. Chávez for providing the core samples from the basement of the Magallanes basin, and F. Escobar and J. Moraga for providing previously unpublished K-Ar and Rb-Sr age determinations. J. Vargas (Universidad de Chile) skilfully separated the zircons. Revisions by Drs. A. Willner, H. Miller and an anonymous referee greatly improved this contribution. We express our gratitude to Dr. A. Demant (Université d'Aix Marseille III) who helped with the microprobe analysis and to Dr. H. Massonne who helped with the necessary subtilities for the Pseudosection calculation.

References

Adie, R.J. 1962. The geology of Antarctica. *In* Antarctic Research: the Matthew Fontaine Maury Memorial Symposium (Wexler, H.; Rubin, M.J.; Caskey, J.E.; editors). American Geophysics Union. Monograph 7: 26-39.

Augustsson, C.; Bahlburg, H. 2007. Provenance of Late Palaeozoic metasediments of the Patagonian proto-

Pacific margin (southernmost Chile and Argentina). International Journal of Earth Sciences (Geologische Rundschau). DOI 10.1007/s00531-006-0158-7.

Biddle, K.T.; Uliana, M.A.; Mitchum, R.M.Jr.; Fitzgerald, M.G.; Wright, R.C. 1986. The stratigraphic and structural evolution of the central and eastern Magallanes Basin, southern South America. *In* Foreland basins (Allen, P.A.; Homewood, P.; editors). International Association of Sedimentologists, Special Publication 8: 41-61.

Black, L.P.; Kamo, S.L.; Allen, C.M.; Aleinikoff, J.N.; Davis, D.W.; Korsch, R.J.; Foudoulis, C. 2003. TEMORA 1: a new zircon standard for Phanerozoic U-Pb geochronology. Chemical Geology 200: 155-170.

Cawood, P.A. 2005. Terra Australis orogen: Rodinia breakup and development of the Pacific and Iapetus margins of Gondwana during the Neoproterozoic and Paleozoic. Earth-Science Reviews 69: 249-279

Connolly, J.A.D. 1990. Multivariable phase diagrams; an algorithm based on generalized thermodynamics. American Journal of Science 290: 666-718.

Connolly, J.A.D. 2005. Computation of phase equilibria by linear programming: A tool for geodynamic modeling and its application to subduction zone decarbonation. Earth and Planetary Science Letters 236: 524-541.

Dalziel, I.W.D. 1997. Neoproterozoic-Paleozoic geography and tectonics: Review, hypothesis, environmental speculation. Geological Society of America Bulletin 109: 16-42.

Faúndez, V.; Hervé, F.; Lacassie, J.P. 2002. Provenance studies of pre-late Jurassic metaturbidite successions of the Patagonian Andes, southern Chile. New Zealand Journal of Geology and Geophysics 45 (4): 411-425.

Fildani, A.; Weislogel, A.; Drinkwater, N.J.; McHargue, T.; Tankard, A.; Joe Wooden, J.; Hodgson, D.; Flint, S. 2009. U-Pb zircon ages from the southwestern Karoo Basin, South Africa-Implications for the Permian-Triassic boundary. Geology 37 (8): 719-722.

Flowerdew, M.J.; Millar, I.L.; Curtis, M.L.; Vaughan, A.P.M.; Horstwood, M.S.A.; Whitehouse, M.J.; Fanning, C.M. 2007. Combined U-Pb geochronology and Hf isotope geochemistry of detrital zircons from early Paleozoic sedimentary rocks, Ellsworth-Whitmore Mountains block, Antarctica. Geological Society of America Bulletin 119 (3/4): 275-288.

Ghidella, M.E.; Yáñez, G.; LaBrecque, J.L. 2002. Revised tectonic implications for the magnetic anomalies of the western Weddell Sea. Tectonophysics 347: 65-86.

Glen, R.A. 2005. The Tasmanides of eastern Australia. *In* Terrane Processes at the Margins of Gondwana (Vaughan, A.P.M.; Leat, P.L.; Pankhurst, R.J.; editors). Geological Society, London, Special Publications 246: 23-96.

Groenewald, P.; Grantham, G.; Watkeys, M. 1991. Geological evidence for a Proterozoic to Mesozoic link between southeastern Africa and Dronning Maud Land, Antarctica. Journal of the Geological Society of London 148: 1115-1123.

Halpern, M. 1973. Regional Geochronology of Chile south of 50°latitude. Geological Society of America Bulletin 84: 2407-2422.

Harambour, S.M. 1998. Structural evolution of the Magallanes Block, Magallanes (Austral) Basin, offshore Argentina, South Atlantic. M.Sc.Thesis (Unpublished), University of London, Royal Holloway New College: 136 p.

Hervé, F.; Fanning, C.M.; Pankhurst, R.J. 2003. Detrital Zircon Age Patterns and Provenance in the metamorphic complexes of Southern Chile. Journal of South American Earth Sciences 16: 107-123.

Hervé, F.; Miller, H.; Pimpirev, C. 2006. Patagonia-Antarctica connections before Gondwana break-up. *In* Antarctica: Contributions to global earth sciences (Fütterer, D.K.; Damaske, D.; Kleinschmidt, G.; Miller, H.; Tessensohn, F.; editors). Heidelberg (Springer): 215-226.

Hervé, F.; Fanning, C.M.; Pankhurst, R.J.; Mpodozis, C.; Klepeis, K.; Calderón, M.; Thomson, S. 2010. Detrital zircon SHRIMP U-Pb age study of the Cordillera Darwin Metamorphic Complex, Tierra del Fuego: sedimentary sources and implications for the evolution of the Pacific margin of Gondwana. Journal of the Geological Society of London 167: 555-568.

Holland, T.J.B.; Powell, R. 1998. An internally consistent thermodynamic data set for phases of petrological interest. Journal of Metamorphic Geology 16: 309-343.

Jacobs, J.; Thomas, R.J.; Armstrong, R.A.; Henjes-Kunst, F. 1999. Age and thermal evolution of the Mesoproterozoic Cape Meredith Complex, West Falkland. Journal of the Geological Society of London 156: 917-928.

König, M.; Jokat, W. 2006. The Mesozoic breakup of the Weddell Sea. Journal Geophysical Research 111: B12102, doi:10.1029/2005JB004035.

Kraus, S. 2007. A hitherto unknown occurrence of crystalline basement cobbles at Paradise Bay, Antarctic Peninsula. GEOSUR 2007. *In* International Geological Congress on the Southern Hemisphere (Demant, A.; Hervé, F.; Menichetti, M.; Tassone, A.; editors), Abstracts Volume: p. 85. Santiago, Chile.

LaBrecque, J.L.; Barker, P. 1981. The age of the Weddell Basin. Nature 290: 489-492.

LaBrecque, J.L.; Ghidella, M.E. 1997. Bathymetry, depth to magnetic basement, and sediment thickness estimates from aerogeophysical data over the western Weddell Sea. Journal of Geophysical Research 102: 7929-7945.

Lawver, L.A.; Gahagan, L.M.; Coffin; M.F. 1992. The development of paleo-seaways around Antarctica. Antarctic Research Series 56: 7-30.

Ludwig, K.R. 2001. SQUID 1.02. A User's Manual.Berkeley Geochronology Center, Special Publication 2: 2455 Ridge Road, Berkeley, CA 94709, USA.

Ludwig, K.R. 2003. User's manual for Isoplot 3.00, a geochronological toolkit for Microsoft Excel. Berkeley Geochronological Centre, Special Publication 4: 71 p.

Massonne, H.J.; Willner, A.; Gerya, T. 2007. Densities of metapelitic rocks at high to ultrahigh pressure conditions: what are the geodynamic consequences? Earth and Planetary Science Letters 256: 12-27.

Millar, I.L.; Pankhurst, R.J. 1987. Rb-Sr geochronology of the region between the Antarctic Peninsula and the Transantarctic Mountains: Haag Nunataks and Mesozoic Granitoids. *In* Gondwana Six: Structure, Tectonics and Geophysics (Mackenzie, G.; editor). American Geophysical Union, Geophysical Monograph 40: 151-160. Washington.

Millar, I.L.; Pankhurst, R.J.; Fanning, C.M. 2002. Basement chronology of the Antarctic Peninsula: recurrent magmatism and anatexis in the Palaeozoic Gondwana margin. Journal of the Geological Society of London 159: 145-157.

Pankhurst, R.J.; Riley, T.R.; Fanning, C.M.; Kelley, S.P. 2000. Episodic silicic volcanism in Patagonia and the Antarctic Peninsula: chronology of magmatism associated with the break-up of Gondwana. Journal of Petrology 41: 605-625.

Pankhurst, R.J.; Rapela, C.W.; Loske, W.P.; Márquez, M.; Fanning, C.M. 2003. Chronological study of the pre-Permian basement rocks of southern Patagonia. Journal of South American Earth Sciences 16: 27-44.

Pankhurst, R.J.; Rapela, C.W.; Fanning, C.M.; Márquez, M. 2006. Gondwanide continental collision and the origin of Patagonia. Earth-Science Reviews 76: 235-257.

Pezzuchi, H. 1978. Estudio geológico de la zona de Estancia Dos Hermanos-Estancia 25 de Marzo y adyacentes, departamento Deseado, Provincia de Santa Cruz. Ph.D. Thesis (Unpublished), Universidad Nacional de La Plata: 99 p. Argentina.

Powell, R.; Holland, T. 1999. Relating formulations of the thermodynamics of mineral solid solutions: Activity modeling of pyroxenes, amphiboles and micas. American Mineralogist 84: 1-14.

Ramos, V.R. 1988. Tectonics of the Late Proterozoic-Early Paleozoic: a collisional history of Southern South America. Episodes 11: 168-174.

Ramos, V.R. 2008. Patagonia: A paleozoic continent adrift? Journal of South American Earth Sciences 26: 235-251.

Rapela, C.W.; Casquet, C.; Baldo, E.; Dahlquist, J.; Pankhurst, R.J.; Galindo, C.; Saavedra, J. 2001. Lower Paleozoic orogenies at the proto Andean margin of South America, Sierras Pampeanas, Argentina. Journal of Iberian Geology 27: 23-41.

Rapela, C.W.; Pankhurst, R.J.; Fanning, C.M.; Grecco, L.E. 2003. Basement evolution of the Sierra de la Ventana Fold Belt: new evidence for Cambrian continental rifting along the southern margin of Gondwana. Journal of the Geological Society of London 160: 613-628.

Rubatto, D. 2002. Zircon trace element geochemistry: partitioning with garnet and the link between U-Pb ages and metamorphism. Chemical Geology 184: 123-138.

Söllner, F.; Miller, H.; Hervé, M. 2000. An Early Cambrian granodiorite age from the pre-Andean basement of Tierra del Fuego (Chile): the missing link between South America and Antarctica? Journal of South American Earth Sciences 13: 163-177.

Suárez, M. 1976. Plate-tectonic model for southern Antarctic Peninsula and its relation to southern Andes. Geology 4 (4): 211-214.

Vavra, G.; Gebauer, D.; Schmid, R.; Compston, W. 1996. Multiple zircon growth and recrystallization during polyphase Late Carboniferous to Triassic metamorphism in granulites of the Ivrea Zone (Southern Alps): An ion microprobe (SHRIMP) study. Contributions to Mineralogy and Petrology 122: 337-358.

Vennum, W.R.; Gizycki, P.; Samsonov, V.V.; Markovich, A.G.; Pankhurst, R.J. 1992. Igneous petrology and geochemistry of the southern Heritage Range, Ellsworth Mountains, West Antarctica. *In* Geology and paleontology of the Ellsworth Mountains, West Antarctica (Webers, G.F.; Craddock, C.; Splettstoesser, J.F.; editors). Geological Society of America Memoir 170: 295-324.

Williams, I.S. 1998. U-Th-Pb geochronology by Ion Microprobe. *In* Applications of microanalytical techniques to understanding mineralizing processes (Mc Kibben, M.A.; Shanks, W.C.; Ridley, W.I.; editors). Reviews in Economic Geology 7: 1-35.

Manuscript received: August 5, 2009; revised/accepted: January 20, 2010.